THREE-DIMENSIONAL LIVE IMAGING OF BOVINE EMBRYOS BY OPTICAL COHERENCE TOMOGRAPHY AND ITS APPLICATION FOR EMBRYO TRANSFER

（光干渉断層撮像法を用いたウシ胚の 3D ライヴイメージングと胚移植における応用に関する研究）

The United Graduate School of Veterinary Science

Yamaguchi University

Yasumitsu Masuda

September 2021

PREFACE

The experiments described in this dissertation were carried out at the Joint Department of Veterinary Medicine, Tottori University, Japan, from April 2019 to March 2021, under the supervision of Associate Professor R. Nishimura.

This dissertation has not been submitted previously whole or in part to a council, a university or any other professional institution for degree, diploma or other professional qualification.

Yasumitsu Masuda

September, 2021

CONTENTS

CHAPTER I

GENERAL INTRODUCTION

Bovine embryo transfer (ET) has been widely used to produce calf in combination with other reproductive technologies, such as *in vitro* fertilization (IVF). However, the conception rate of ET using IVF embryos (30-40%) is lower than that using embryos produced *in vivo* (around 50%) [1-4]. Embryos for transfer are usually selected by observation under a conventional optical microscope at the time of transfer, and embryo quality is subjectively assigned one of the codes according to the International Embryo Technology Society (IETS) standards for embryo evaluation [5, 6].

In human artificial reproductive technology (ART), embryos are evaluated based on Veeck and Gardner classification [7, 8], and time-lapse cinematography (TLC) with a visible light microscope has recently become a popular technology. Morphokinetic parameters, such as the number of pronuclei or nuclei, timing of cleavage and the number of blastomeres, are used as potential indicators that may improve the success of ART [9]. Furthermore, ART success rate has been improved by comprehensive chromosomal screening, using techniques such as array comparative genomic hybridization, quantitative single nucleotide polymorphism arrays and next-generation sequencing [10, 11]. To evaluate *in vitro* developed bovine embryos, TLC has been used to determine the time of the first cleavage and the subsequent number of blastomeres, and the number of blastomeres at the onset of the lag-phase [4, 12-14]. However, so far, live bovine embryos have not been evaluated based on their three-dimensional (3D) structure.

A morphological grading system in human ART, first described by Gardner and Schoolcraft [15]. According to this system, three parameters (degree of blastocoel expansion, size and compactness of inner cell mass (ICM), and the cohesiveness and number of trophectoderm (TE)) are graded. Based on this grading criteria, an additional consensus on embryo assessment was agreed including new references for each parameter [16, 17]. In this consensus, ICM grade is suggested to be more important for determining the implantation potential of blastocysts. To select the best blastocyst when performing ET on Day 5, several parameters have been suggested to contribute to the implantation potential of blastocysts. Some investigators have shown that timing of blastocoel development and grade of expansion are important parameters for implantation [18-20]. Other investigators have suggested that size and shape of ICM are related to implantation [21-23]. Either a positive association or no association of TE cells with implantation have been reported [22, 24-26]. Although morphological grading in human blastocysts has been much reported above, that in bovine blastocysts are recognized to be more difficult because of their dark cytoplasm [27, 28].

Optical coherence tomography (OCT) has been developed for non-invasive, cross-sectional imaging in biological systems [29-31], and is presently used in ophthalmology, especially for funduscopic examination of the retina. OCT can be used to measure 3D images with high spatial resolution, so that it can scan small biological structures, such as micro vessel structures during *in vitro* angiogenesis [31]. Recently, OCT imaging of mouse [32-34] and porcine [34] early-stage embryo has been reported. In the mouse blastocysts, their nucleoli were also clearly visualized by OCT [34]. In cattle, blastocysts have been imaged by OCT, and

monitored their cytoplasm movements potencially associated with viability, suggesting that OCT can be used for the masurement of the damage after cryopreservation [35]. However, the quantification of structures of bovine blastocysts for evaluating embryo quality has not been reported. We have recently developed a technique for 3D imaging of bovine blastocysts, and used it to evaluate 22 parameters including the volumes of ICM, TE, ZP and blastocoel of an embryo [36]. Here, we used this technique to compare the characteristics of embryos that did or did not develop to term, in order to identify parameters associated with successful ET. Furthermore, in the blastomere observation, shape, size, cytoplasm color, even distribution of cytoplasm, and the number of nucleus have been suggested to be related to developmental potential of bovine embryos [4, 12-14]. Because bovine and porcine early embryos contain much more lipid than human or mouse embryos, pronucleus formation in early embryos cannot be confirmed under a microscope, which make it difficult to evaluate their quality [27, 28, 37, 38]. Thus, we have also tried to obtain 3D images of early-stage bovine embryos.

CHAPTER II

THREE-DIMENSIONAL LIVE IMAGING OF BOVINE EMBRYOS BY OPTICAL COHERENCE TOMOGRAPHY

OBJECT OF THE STUDY

In CHAPTER II, to establish a new method for evaluation of bovine embryo for ET, we tried to take non-invasive, cross-sectional 3D images of external form and internal structure of bovine blastocyst by using the OCT system and quantified several parameters based on the OCT-detected 3D images.

MATERIALS & METHODS

Ethics Statement

Animal handling and experimental procedures were carried out following the Guidelines for Proper Conduct of Animal Experiments by Science Council of Japan (http://www.scj.go.jp/ja/info/kohyo/pdf/kohyo-20-k16-2e.pdf).

Experimental Design

Bovine IVF embryos were derived from oocytes obtained by ovum pick-up (OPU) and were cryopreserved until the time of ET. We investigated their morphological structures by OCT and determined their fertility following transfer into recipient cattle.

Production of Embryos Derived from Oocytes Collected by OPU and in Vitro

Maturation (IVM).

As previously described [39], cumulus-oocyte complexes (COCs) were collected from a 73-month-old Japanese Black cow using an ultrasound scanner (HS-2100; Honda Electronics, Toyohashi, Japan) and a 7.5-MHz convex array transducer (HCV-4710MV; Honda Electronics) with a 17-gauge stainless steel needle guide. Follicles > 2 mm in diameter were aspirated with the vacuum through a disposable aspiration needle (COVA Needle; Misawa Medical, Tokyo, Japan). The aspiration rate was 14 mL/min, and the vacuum pressure was 100 mmHg. The IVM medium was 25 mM HEPES-buffered TCM199 (M199; Gibco, Paisley, Scotland, UK), supplemented with 10% newborn calf serum (NCS; 16010159, Gibco) and 0.01 AU/mL follicle-stimulating hormone from porcine pituitary (Antorin-R10; Kyoritsu Seiyaku, Tokyo, Japan). COCs with two or more granulosa layers were washed thrice with IVM medium, and the recovered COCs were cultured in four-well dishes (Non-Treated Multidishes; Nalge Nunc International, Roskilde, Denmark) in 600 µL of IVM medium. The cultures were covered with mineral oil (M8414; Sigma-Aldrich, St. Louis, MO, USA) and incubated for 21–22 h at 38.5°C in 5% CO_2, 5% O_2, and 90% N_2 with humidified air. All cultures were maintained under these conditions.

IVF

Frozen semen from Japanese Black bulls stored in straws was thawed in water at 37°C for 40 sec. After centrifugation (840 ×*g*, 5 min), the supernatant was removed and the sperm suspension with a final sperm concentration of 1.0×10^7/mL diluted by IVF100 (Research Institute for the Functional Peptides, Yamagata, Japan) served as the IVF medium. After 22 h of IVM, the COCs were removed from

the IVM medium and washed twice with IVF100. Up to 20 COCs were incubated in 35 mm dishes (Falcon 351008; Corning, NY, USA) containing 100 µL droplets of IVF medium for 6 h.

in Vitro Culture (IVC)

After insemination, oocytes were completely denuded from cumulus cells and spermatozoa by repeated pipetting with a glass pipette in the IVC medium, potassium simplex optimized medium (KSOM) with amino acid (KSOMaa Evolve Bovine; Zenith Biotech, Bangkok, Thailand) supplemented with 5% NCS and 0.6 mg/mL L-carnitine (C0158, Sigma-Aldrich). Presumptive zygotes were subsequently washed thrice with IVC medium and cultured for 48 h in 100 µL droplets of IVC medium. Each droplet contained approximately 20 presumptive zygotes. At 48 hpi, embryos with more than four cells were transferred from 35 mm dishes to well-of-the-well (WOW) dishes (LinKID micro25, Dai Nippon Printing Co., Ltd., Tokyo, Japan) as previously described [12]. WOW dishes, which are 35 mm in diameter, have 25 microwells (5 columns × 5 rows) and a circular wall in the center. A WOW dish can culture up to 25 embryos each with a single drop of medium, and allows tracking of individual embryos. Pre-cultured IVC medium (100 µL) was placed within the circular wall and covered with mineral oil. At 168 to 180 hpi, embryos that had developed to or beyond the blastocyst stage were observed under an inverted microscope.

OCT Observations

IVF embryos were cultured for 7 days (such that they had reached the

expanded blastocyst stage) and examined under an inverted microscope. Only embryos that were independently classified as IETS Code 1 by three skilled observers were used. OCT imaging was performed as previously described [31].

Unstained live embryos were imaged by OCT using a Cell3iMager Estier (SCREEN Holdings Co., Ltd., Kyoto, Japan). Values for multiple parameters based on the Gardner classification were obtained from the 3D image data. The system is equipped with a superluminescent diode (SLD; center wavelength: 890 nm, N.A. = 0.3). The SLD output is coupled to a single-mode optical fiber and split at an optical fiber coupler into the sample and reference arms. The reflections from the two arms were combined at the coupler and detected by a spectrometer. The 3D image data of the embryos were constructed from individual 2D x–z cross-sectional images, which were obtained by a series of longitudinal scans by laterally translating the optical beam position. The data acquisition window was 200–300 × 200–300 × 200–300 µm, and the voxel size was 1 × 1 × 1 µm (Figure 1).

Cryopreservation

As described previously [40], blastocysts imaged by OCT were transferred to a cryoprotective solution (1.8 M ethylene glycol and 0.1 M sucrose in Dulbecco's PBS), which was then placed in a 0.25 mL straw (IMV Technologies, L'Aigle, France) at room temperature (25°C). After the blastocysts were equilibrated at room temperature for 15 min, the straws were directly set in a programmable freezer (ET-1N; FUJIHIRA INDUSTRY CO., LTD., Tokyo, Japan) at –7°C where seeding was manually performed. The straws were subsequently cooled at a rate of 0.3°C/min to –30°C and then directly transferred to liquid nitrogen for storage until use. The

straws were thawed in air for 10 sec and then immersed in a water bath at 30°C for 20 sec for ET.

Image Analysis

The image analysis process is briefly shown in Figure 3. The 3D images of bovine embryos were binarized. The binarized image was separated into ICM, TE, and ZP. The thickness of the embryo (T_{ALL}) was measured by drawing vectors from the center to the outer surface and inner surface (the outermost of blastocoel) of the embryo in the elevation direction (–90 to 90 degrees) and the azimuth direction (–180° to 180°). ICM parts were extracted from T_{ALL} by Otsu's thresholding method [41, 42]. The parts that remained after removing ICM parts from T_{ALL} were defined as T_{other}. T_{other} were separated using the Otsu's thresholding method into TE and ZP by calculating their average thickness [41, 42].

ET and Pregnancy Diagnosis.

The OCT-imaged embryos were transferred to seven 3.9 ± 1.2-year-old recipient Holstein cows in February and March 2019 at a commercial farm in Tottori prefecture, Japan. The cows were clinically normal with body condition scores (BSC) between 2.75 and 3.0. The BCS scale ranges from 1 to 5 with 0.25 increments. Before ET, recipients were estrus-synchronized by administration of a CIDR device (CIDR 1900; Zoetis Japan, Tokyo, Japan) for 9 days and treated with cloprostenol (Dalmazin 150 μg im; Kyoritsu Seiyaku Corporation, Tokyo, Japan) 2 days before CIDR removal. The estrus of recipient cows was monitored, and embryos were transferred 7 days after estrus. The recipients were examined for pregnancy 23 days

after ET using ultrasonography (HS101V; Honda Electronics). Pregnancy was confirmed by observation of the embryonic membrane and the embryo with a detectable heart beat in the intraluminal uterine fluid.

RESULTS

3D Imaging of Bovine IVF Embryos

The OCT system scans the light source in the x-axis while shifting the scanning line positions on the y-axis to obtain a signal on the x-y plane at a focus position on the z-axis. We repeated this scanning while shifting z-axis focus positions to obtain 3D images of embryos (Figure 1). The lengths of the imaging range on the x-axis, y-axis, and z-axis were 300, 300, and 200 µm, respectively. The exposure time was 150 µsec, and the scanning of an entire embryo could be completed in a few minutes. OCT provided cross-sectional images with a slice thickness of 1 µm, as shown in Figure 1. OCT allows obtaining live images non-invasively without staining. It was possible to visualize the fine structure inside the embryo that could not be observed with an optical microscope (Figure 2: representative images of an embryo [No. 2 in Table 1]). Before transfer, the embryo was imaged under a microscope (Figure 2A) and by OCT. Based on the OCT images, TE (cyan) and ICM (magenta) were 3D-visualized (Figure 2B). The structure of the whole embryo, including the ICM (red), TE (blue), and zona pellucida (ZP; gray), were also 3D-visualized (Figure 2C). In addition, each part of the embryo, ICM (Figure 2D), TE (Figure 2E), and blastocoel (Figure 2F), was individually 3D-visualized.

Quantification of Bovine Embryo Morphology and ET Success Rate

The values of the 22 parameters measured for the seven embryos are shown in Table 1. In embryos subjected to ET, the average thickness of ICM, TE, ZP, and TE + ZP were 50.9 ± 7.3, 3.8 ± 0.8, 14.3 ± 1.7, and 18.7 ± 1.2 μm, respectively. The average volumes of ICM, TE, ZP, TE + ZP, ICM + TE + ZP, blastocoel, and whole embryo were 3.2 ± 0.4, 2.0 ± 0.6, 15.0 ± 0.2, 17.4 ± 1.9, 20.6 ± 1.6, 12.8 ± 2.3, and 33.4 ± 3.7 × 10^5 μm^3, respectively. The blastocoel diameter was 51.7 ± 2.6 μm. Four of the seven recipients became pregnant.

DISCUSSION

The present results describe the first 3D imaging of bovine embryos using OCT. The images clearly revealed the internal structures of the embryos, otherwise difficult to observe under a microscope. The 3D images could also be used to calculate morphological parameters such as volume of the parts of the embryo (whole, blastocoel, ICM, and TE). These parameters may be useful for evaluating embryo quality before ET. In human ART, several parameters such as embryo development stage, blastocoel volume, ICM, and TE thickness are recognized as assessment criteria. The operator subjectively determines the scores of these parameters by microscopic observation [43, 44]. The present study shows that a stage-top OCT system could serve as a new way of objectively evaluating the quality of bovine embryos. Bovine embryos for ET are usually evaluated by the IETS codes [5, 6] whose accuracy relies on the proficiency of the operators. Sugimura et al. [4, 13] showed that high-quality bovine embryos could be selected using morphokinetic indicators such as timing, number of blastomeres at first cleavage, and number of blastomeres at the onset of the lag phase as well as by observing

nuclear/chromosomal abnormalities of bovine embryos using live-cell imaging technology [45]. Thus, morphological indices contribute to the critical selection of high-quality bovine embryos. Therefore, OCT images that allow observation of morphological details of the internal structure may also be useful to evaluate the quality of bovine embryos. At 168 h post-insemination (hpi), embryos that were classified as IETS Code 1 were used for imaging. embryos contain much more lipids than human or mouse embryos, pronucleus formation in early embryos could not be confirmed under a microscope, posing difficulty in evaluation of their quality [27]. Zheng et al. [32] used OCT to observe the 3D morphology of mouse early embryos (mono-, 2-, and 4-cell stages). These authors succeeded in label-free visualization of the male and female pronucleus before the first cleavage and the nucleus in the blastomere after cleavage [32]. In cattle, OCT imaging of early embryos may be useful for visualizing pronuclei and detecting morphological abnormalities that are difficult to observe using a conventional microscope. The OCT system used in the present study has been suggested to provide effective information for the evaluation of bovine embryos by the precise observation of the 3D structure of the embryo. The present results show OCT images only in the embryos classified as Code 1 of IETS codes. Therefore, OCT evaluation of embryos in other IETS codes is warranted to confirm its applicability for the morphological evaluation of bovine embryos.

Using the OCT system, we could quantify the internal structure of bovine embryos. IETS codes grade embryos according to their developmental stages and the status of degeneration of the cells in the embryo but provide no information about the volume of the whole embryo, ICM, or TE [5]. In human ART, Gardner classification is insufficient for morphological selection of good embryos; however,

morphological parameters of TE have been suggested to be more closely associated with live birth than those of ICM [26]. As morphological parameters of TE were also quantified by OCT in the present study, OCT may support the selection of good bovine embryos for transfer.

The growth potential of early embryos relies on the total cell number of blastocysts, especially the composition ratio of ICM and TE [46]. The number of cells in a bovine embryo is usually counted by double staining with Hoechst 33258 and propidium iodide [46]. However, stained embryos cannot be used for ET. The OCT system uses near-infrared light (λ: 900 nm), which has low cytotoxicity [47–49], and allows non-invasive observations of bovine embryo morphology; therefore, OCT-scanned embryos can be used for ET. We have also used the same OCT system to observe mouse embryos before ET and achieved a normal delivery after ET (Ohbayashi et al., unpublished data). In the present study, we achieved conceptions after transferring bovine embryos imaged by the same OCT system used in mice. A few minutes of OCT did not change the embryo morphology. Together, these findings indicate that using the OCT system could allow visualization of the internal 3D structure and quantification of morphological parameters in living bovine embryos. This new method has the potential to support the objective evaluation of bovine embryos before ET. The comparison of the values of each parameter found in the present study between pregnancy and non-pregnancy is important to determine whether the OCT system is available for embryo evaluation for ET.

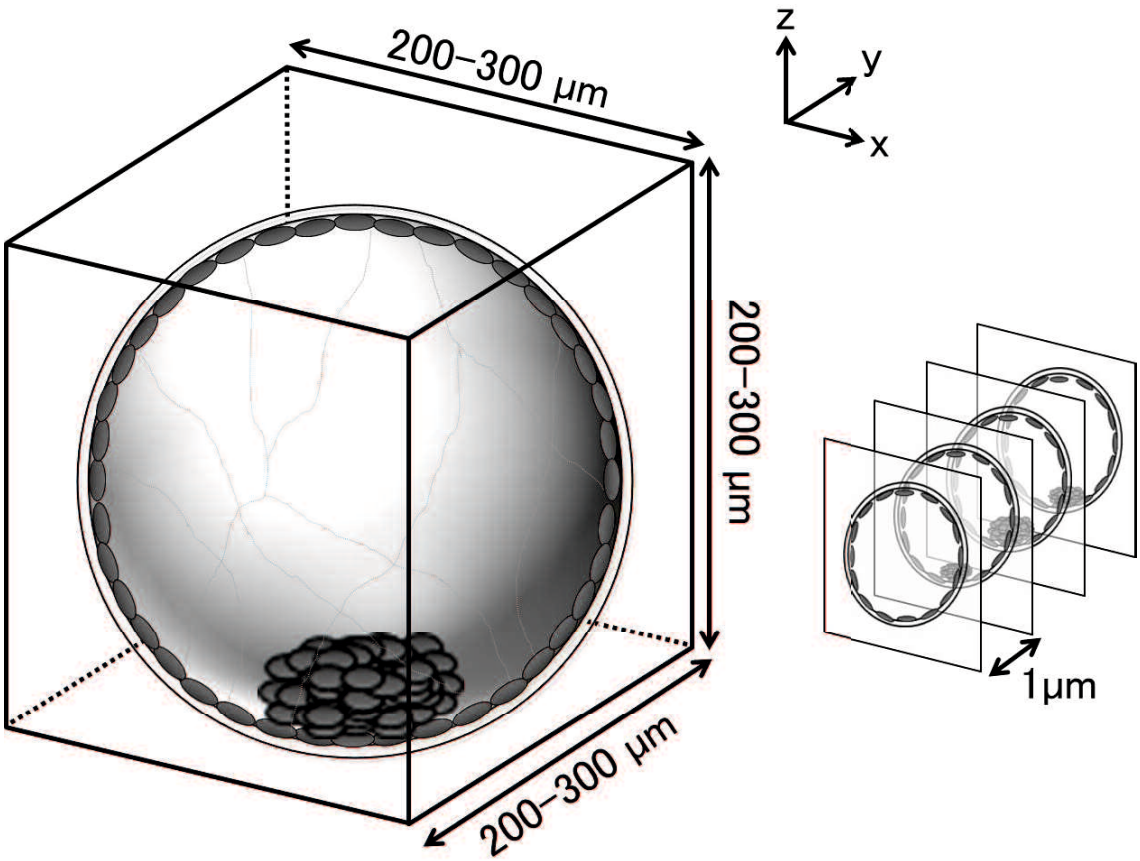

Fig.1 Scanning scale for bovine embryo. Longitudinal imaging was performed in the area of bovine emryo.

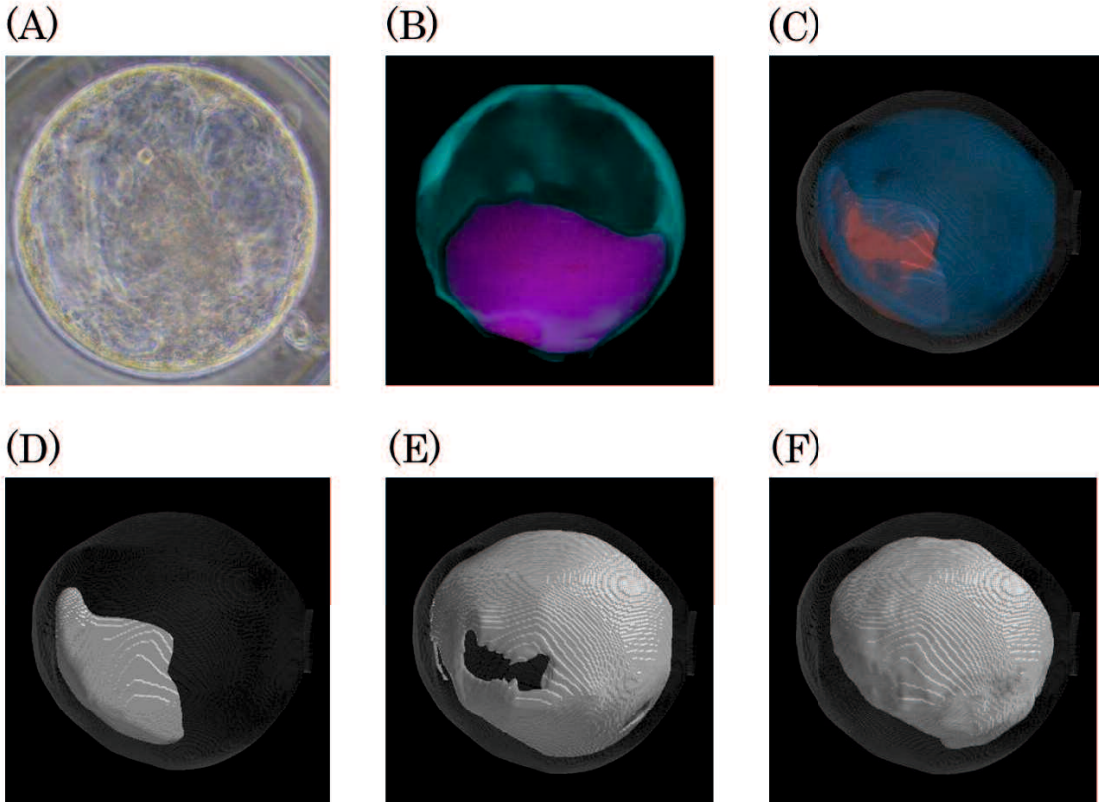

Fig.2 Optical coherence tomography (OCT) images of a transferred bovine embryo (embryo No. 2 in table 1). (A) Transferred embryo imaged by a microscope. This embryo was determined as Code 1 according to the IETS codes. (B) Sum of all pixel values in z-stack images of trophectoderm (TE; cyan) and inner cell mass (ICM; magenta) part was extracted from the tomographic image and synthesized 2D image. (C) 3D visualization of structures of an embryo, including ICM (red), TE (blue), zona pellucida (ZP; gray), and blastocoel. (D-F) 3D visualization of each structure of an embryo: ICM (D), TE (E), and blastocoel (F).

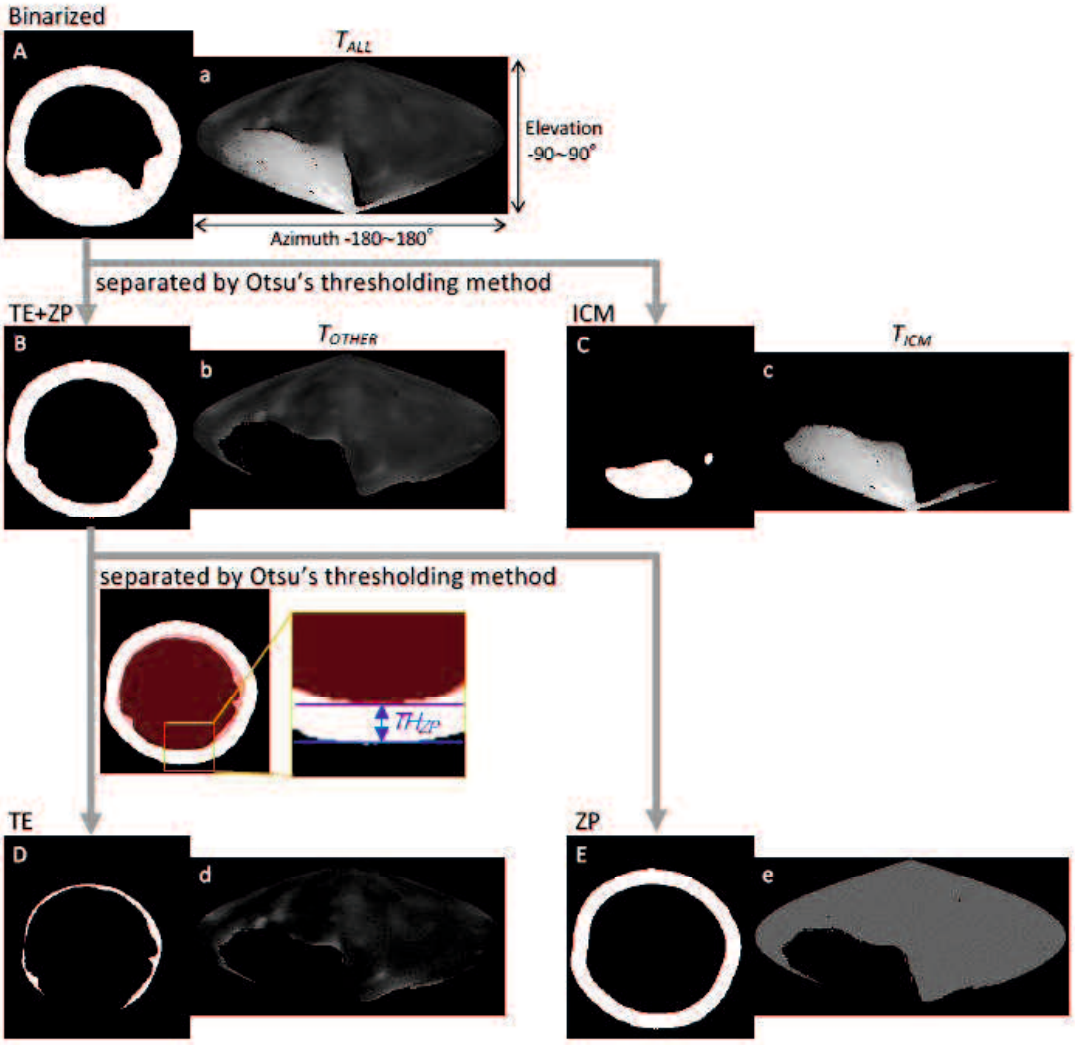

Fig.3 3D image analysis of bovine embryos. The binarized image was separated into inner cell mass (ICM), trophectoderm (TE), and zona pellucida (ZP). (Panel A & a) Thickness of embryo (T_{ALL}) was measured by drawing vectors from center to outer surface and inner surface (the outermost of blastocoel) of the embryo. ICM parts (Panels C & c) were extracted from T_{ALL} by the Otsu's thresholding method. (Panels B & b) The parts that remained after removing ICM parts from T_{ALL} were defined as T_{OTHER}. T_{OTHER} were separated using the Otsu's thresholding method into TE (Panels D & d) and ZP (Panels E & e) by calculating their average thickness. A-E: A 2D image derived from a binarized 3D image. a-e: Sinusoidal projection for each part of a 3D image. TH_{ZP}: Threshold of ZP.

Table 1. Quantification of 22 parameters in bovine embryo (n=7)

		Embryo No.							
		1	2	3	4	5	6	7	mean ± SD
Structual thickness (μm)									
ICM	Mean	38.1	56.2	42.2	53.2	51.8	59.9	55.2	50.9 ± 7.3
	Median	38.0	57.1	43.1	55.0	55.1	61.3	56.2	52.3 ± 7.8
	SD	5.9	8.2	5.5	7.4	9.1	8.5	7.1	7.4 ± 1.3
TE	Mean	3.1	3.7	3.0	4.3	5.0	4.7	3.0	3.8 ± 0.8
	Median	2.5	2.6	2.4	3.1	3.2	3.6	2.5	2.9 ± 0.4
	SD	2.4	3.4	2.6	4.1	5.1	4.3	3.1	3.6 ± 0.9
ZP	Mean	16.4	14.9	16.6	13.3	11.4	13.8	13.6	14.3 ± 1.7
	Median	17.0	15.4	17.1	13.4	12.0	15.0	14.3	14.9 ± 1.7
	SD	2.5	2.1	2.6	1.9	1.8	3.0	3.0	2.4 ± 0.5
TE + ZP	Mean	19.7	19.4	19.6	17.7	16.7	19.8	17.9	18.7 ± 1.2
	Median	19.9	19.0	19.5	17.0	15.1	19.1	18.0	18.2 ± 1.6
	SD	3.9	3.8	4.0	4.8	5.3	4.9	4.1	4.4 ± 0.6
Volume ($\times 10^5$ μm^3)									
	ICM	2.5	3.1	2.7	3.6	3.7	3.3	3.6	3.2 ± 0.4
	TE	1.2	2.4	1.4	1.8	2.6	2.7	1.7	2.0 ± 0.6
	ZP	16.2	14.4	20.0	13.7	11.9	14.8	13.9	15.0 ± 0.2
	TE + ZP	17.5	17.4	21.4	16.0	15.5	18.1	16.0	17.4 ± 1.9
	ICM + TE + ZP	20.0	20.5	24.1	19.6	19.2	21.5	19.5	20.6 ± 1.6
	Blastocoel	11.4	11.3	18.1	12.0	13.8	11.5	11.2	12.8 ± 2.3
	Whole embryo	31.4	31.9	42.2	31.5	33.0	33.0	30.7	33.4 ± 3.7
Diameter of blastocoel (μm)									
	Mean	49.3	50.7	57.6	50.7	53.2	50.3	50.4	51.7 ± 2.6
	Median	51.6	52.7	60.3	52.9	55.7	52.5	52.4	54.0 ± 2.8
	SD	13.3	14.5	15.6	14.1	14.8	14.1	14.5	14.4 ± 0.7
ET status									
	IETS Code	Code 1	Code 1	Code 1	Code 1	Code 1	Code 1	Code 1	
	Pregnancy	–	+	+	+	–	+	–	

ICM, inner cell mass; TE, trophectoderm; ZP, zona pellucida.

CHAPTER III

THREE-DIMENSIONAL LIVE IMAGING OF BOVINE PREIMPLANTATION EMBRYOS

OBJECT OF THE STUDY

In CHAPTER III, to evaluate the developmental potential of bovine preimplantation embryos, we have used the non-invasive method of OCT to obtain live images of embryos at 2-cell and blastocyst stages. The images were used to confirm the number of nucleus in 2-cell stage embryos and to evaluate the morphological parameters, such as the volumes of the ICM and the thicknesses of the TE, in blastocyst stage embryos.

MATERIALS & METHODS

Ethics Statement

Animal handling and experimental procedures were carried out following the Guidelines for Proper Conduct of Animal Experiments by the Science Council of Japan (http://www.scj.go.jp/ja/info/kohyo/pdf/kohyo-20-k16-2e.pdf).

Production of Embryos Derived from Oocytes Collected by OPU and in Vitro Maturation (IVM).

As described previously (39), COCs were collected from Japanese Black cows (n = 12; 110.4 ± 34.3-month-old) by OPU using an ultrasound scanner (HS-2100; Honda Electronics) and a 7.5-MHz convex array transducer (HCV-4710MV; Honda

Electronics) with a 17-gauge stainless steel needle guide (242 COCs, in total). Follicles >2mm in diameter were aspirated with a vacuum through a disposable aspiration needle (COVA Needle; Misawa Medical). The aspiration rate was 14 mL/min and the vacuum pressure was 100 mmHg. The IVM medium was 25mM HEPES-buffered TCM199 (M199; Gibco), supplemented with 10% NCS (16010159, Gibco) and 0.01 AU/mL of follicle-stimulating hormone from porcine pituitary (Antorin-R10; Kyoritsu Seiyaku). COCs with two or more granulosa layers were washed three times with IVM medium. Recovered COCs were cultured in 4-well dishes (Non-Treated Multidishes; Nalge Nunc International) in 600 µL of IVM medium, covered with mineral oil (M8414; Sigma-Aldrich), and incubated for 22 h at 38.5°C in 5% CO_2, 5% O_2, and 90% N_2 in humidified air. All cultures were maintained under these conditions.

IVF

Frozen semen of Japanese Black bulls stored in straws was thawed in water (37°C, 40 sec), and then centrifuged twice in IVF100 (Research Institute for the Functional Peptides; 600 ×*g*, 5 min). After centrifugation, spermatozoa were removed from the pellet, and added to IVF100 to obtain a suspension with a final sperm concentration of 1.0×10^7/mL. This suspension served as the IVF medium. After 22 h of IVM, the COCs were washed twice with IVF100. Up to 20 COCs were incubated in 100 µL droplets of IVF medium in 35mm dishes (Falcon 351008; Corning) for 6 h.

IVC

After insemination, oocytes were completely denuded from the cumulus cells and spermatozoa by pipetting with a glass pipette in IVC medium: (KSOMaa Evolve Bovine; Zenith Biotech) supplemented with 5% NCS and 0.6 mg/mL of L-carnitine (C0158, Sigma-Aldrich). Subsequently, presumptive zygotes were washed three times with IVC medium and cultured in 100 µL droplets of IVC medium for 48 h. Each droplet contained approximately 20 presumptive zygotes. Average value of cleavage rate was 74.0% (179/242). At 48 h post-insemination (hpi), embryos with more than four cells were transferred from the 35mm dishes to WOW dishes (LinKID micro25, Dai Nippon Printing Co., Ltd) as described [12]. In order to track individual embryos throughout the culture. IVC medium and mineral oil were pre-cultured for at least 12 h in glass bottles separately at 38.5°C in 5% CO_2, 5% O_2, and 90% N_2 in humidified air, and the was placed within the circular wall and covered with the pre-cultured mineral oil. At 168 to 180 hpi, embryos that had developed to or beyond the blastocyst stage were observed under an inverted microscope. Finally, 123 embryos had developed to the blastocyst stage (50.8%), and 80 blastocysts had been cryopreserved.

OCT Observations

IVF embryos were cultured for seven days (by this time, they reached the expanded blastocyst stage) and examined under an inverted microscope at 27–31 hpi (at the 2-cell stage; n = 15) and at 168 to 180 hpi (at the blastocyst stage; n = 30). In blastocysts, only the embryos that were independently classified as Code1 according to the IETS standards by three skilled observers were used. OCT imaging was done as described previously (31, 36). Unstained live embryos were imaged by OCT using

the Cell3iMager Estier (SCREEN Holdings Co., Ltd). The imaging system of Cell3iMager Estier is outlined in Figure 1. The system is equipped with a SLD (center wavelength: 890 nm, N.A. = 0.3). The SLD output is coupled to a single-mode optical fiber and split at an optical fiber coupler into the sample and reference arms. The reflections from the two arms are combined at the coupler and detected by the spectrometer. The 3D image data of the blastocysts were constructed from individual 2D ×-z cross-sectional images, which were obtained by a series of longitudinal scans obtained by laterally translating the optical beam position. The data acquisition window was 200–300 × 200–300 × 200–300 µm, and the voxel size was 1 × 1 × 1 µm. The OCT system scans light source positions in the x-axis direction while the shifting scanning line positions on the y-axis to obtain a signal on the x–y plane at a focus position on the z-axis. By repeating this scanning while shifting the z-axis focus positions, 3D images of the embryos were acquired. The lengths of the imaging range on the x-, y-, and z-axis were 300, 300, and 200 µm, respectively. The exposure time was 150 µsec, and scanning an entire embryo was completed in a few minutes. OCT provided cross-sectional images with a slice thickness of 1 µm.

Cryopreservation

As described previously [40], blastocysts imaged by OCT were transferred to a cryoprotective solution (1.8 M of ethylene glycol and 0.1 M of sucrose in Dulbecco's PBS), which was then placed in a 0.25-mL straw (IMV Technologies, L'Aigle) at room temperature. After the blastocysts were equilibrated at room temperature for 15 min, the straws were directly set in a programmable freezer (ET-1N; FUJIHIRA INDUSTRY CO., LTD) at −7°C where seeding was manually

performed. Subsequently, the straws were cooled at a rate of 0.3°C/min to −30°C and then directly transferred to liquid nitrogen for storage until use. The straws were thawed in air for 10 sec and then immersed in water (30°C, 20 sec) for the ET. Because of the status of our farms, we have chosen a cryopreservation protocol rather than a verification protocol.

Image Analysis

We recently reported using OCT to image bovine embryos [36]. After the 3D images were captured by OCT (Figure 4), the 3D images were analyzed in an automized way (Figures 5, 6). Process (i) The 3D images of bovine embryos were binarized (Figures 5, 6). For each image, vectors were drawn at equal angles in the elevation direction (−90–90°) and the azimuth direction (−180–180°) from the center of the embryo to the outer surface and the inner surface (the outermost of blastocoel). The thicknesses of the embryo along each vector (T_{All}) were then measured (Figure 3). Process (ii) To distinguish the ICM from T_{All}, an appropriate threshold (TH_{icm}; the cut-off value for distinguishing ICM from T_{All}) was set by Otsu's method [41, 42] (Figure 3). The parts where the thickness from the outer edge of the embryo region was lower than TH_{icm} were excluded from the binarized images. The largest object among the remaining objects after the exclusion was defined as ICM. T_{ALL} was separated into the thickness information of the area corresponding to ICM (T_{ICM}) and the thickness information areas other than ICM (T_{other}). Process (iii) Based on the T_{other} value, the average thickness (TH_m) was evaluated, and the threshold (TH_t) was set by Otsu's method [41, 42] (Figure 3). The threshold (TH_{zp}) that separates TE and

ZP was set by TH_m–(TH_t- TH_m) (in case of $TH_t > TH_m$) or by TH_m + (TH_m- TH_t) (in case of $TH_m \geqq TH_t$). The region where the thickness of T_{other} was lower than TH_{zp} was defined as ZP, and the remaining region after removing TH_{zp} from T_{other} was defined as TE. The unfulfilled region, surrounded by the embryo parts, such as ICM, ZP, and TE, in the binarized image was defined as the blastocoel. The volumes of the defined ICM, TE, ZP, and blastocoel were evaluated. The means, medians, standard deviations, minimum, maximum, and range of the thickness of ICM were evaluated from T_{ICM}. The thickness of TE was evaluated from the thickness information, which was obtained by subtracting TH_{zp} from T_{other}. Summary statistics related to the thickness of ZP was set by TH_{zp}.

ET and Pregnancy Diagnosis

The OCT-imaged embryos were transferred to 30 recipient cows [47.5 ± 25.5-month-old Holstein (18 lactating cows) and Japanese Black cows (10 cows; two cows received ET twice)] from March 2018 to February 2019 at the farms in Tottori prefecture, Japan. The cows were clinically normal with BCS between 2.75 and 3.0 (BCS scale goes from 1 to 5 with 0.25 increments). Before ET, recipients were estrus-synchronized by the administration of a CIDR device (CIDR 1900; Zoetis Japan) for 9 days and a treatment with cloprostenol (Dalmazin 150 μg [i.m.]; Kyoritsu Seiyaku Corporation) 2 days before the CIDR removal. Estrus of recipient cows was monitored, and embryos were transferred seven days after estrus with the confirmation of the presence of corpus luteum (CL; diameter ≧ 20 mm). The recipients were examined for pregnancy 23 days after ET using ultrasonography (HS101V; Honda Electronics). Pregnancy was confirmed in nine Holstein cows and

six Japanese Black cows by observation of a CL ≧ 20 mm in diameter and an embryo with a detectable heartbeat in the intraluminal uterine fluid and an embryonic membrane. Ages of pregnant and non-pregnant cows were 42.3 ± 19.9 and 52.7 ± 29.5-months-old, respectively. Cows with BCS of 2.75 and 3.0 were included equally in both pregnant and non-pregnant cows.

Data Analysis

Hierarchical clustering analysis was performed using 13 blastocoel-related and ZP-related parameters of bovine blastocysts. Metrics and linkage criteria for hierarchical clustering were Pearson's correlation and unweighted average linkage. The data was normalized so that the average = 0 and SD = 1 for each of the parameter. Hierarchical clustering analysis was performed using the SciPy (ver.1.3.0) package in Python (ver.3.6.5). Statistical significance was analyzed using the Mann-Whitney U test. A value of $p < 0.05$ was considered statistically significant. Mann-Whitney U test was performed using the SciPy (ver.1.3.0) package in Python (ver.3.6.5). Principal component analysis (PCA) was performed using 22 parameters of bovine blastocysts. The data was normalized so that the average = 0 and SD = 1 for each of the parameter. PCA was performed using the scikit-learn (ver.0.23.2) package in Python (ver.3.6.5).

RESULTS

3D Imaging of Bovine IVF Embryos at 2-Cell Stage

With OCT, it was possible to non-invasively obtain live 3D images of a 2-cell embryo. OCT images also showed the nuclei (Figures 7B, C), which made it easy

to find binuclear blastomeres (blue and green in Figures 8B, C). Of the 15 embryos examined by OCT, two were binuclear and were not used for transfer.

Quantification of Bovine Embryo Morphology at the Blastocyst Stage and ET Success Rate

Before transfer, we obtained images of an embryo with a microscope (Figures 9A, 10A) and with OCT. OCT images of the trophectoderm (TE) and inner cell mass (ICM) of representative embryos resulting in pregnancy (P embryos) and non-pregnancy (NP embryos) are shown in Figures 9B, 10B, respectively. In these figures, TE and ICM were artificially colored green and orange, respectively. The structure of a whole embryo, including ICM (orange), TE (green), and zona pellucida (ZP; gray) were also 3D-visualized (Figures 9C, 10C). Each part of the embryo, the ICM (Figures 9D, 10D), TE (Figures 9E, 10E), and blastocoel (Figures 9F, 10F), was also 3Dvisualized individually.

Twenty-two parameters were measured for each of the 30 embryos (Table 2). For the embryos that were subjected to ET (n = 30), the average thicknesses of ICM, TE, ZP, and TE + ZP were 55.1 ± 14.1, 4.2 ± 1.2, 15.2 ± 3.4, and 19.5 ± 3.8 μm, respectively (mean ± SD). The average volumes of ICM, TE, ZP, TE + ZP, ICM + TE + ZP, blastocoel, and whole embryo were 3.7 ± 1.3, 2.0 ± 0.9, 16.1 ± 3.5, 18.7 ± 4.0, 22.4 ± 4.7, 13.4 ± 5.5, and 35.8 ± 8.1 × 105 μm^3, respectively (mean ± SD), and the blastocoel diameters were 52.3 ± 7.7 μm (mean ± SD). Fifteen of the 30 recipients became pregnant. None of the parameters were significantly different between the embryos that did (P) or did not (NP) lead to pregnancy (Table 2; Figure 11). Twelve of the 15 pregnant cows gave birth (six males and six females), and the remaining

three cows experienced a late embryonic death. Newborn calves had typical weights (male: 40.2 kg; female: 35.5 kg, in average), and did not show any congenital defects, neonatal overgrowth, and death.

PCA of 22 Morphological Parameters of Bovine Blastocysts

A PCA identified three principal components, PC1, PC2, and PC3. PC1 was related to the thickness of ZP and TE, which accounted for 41.00% of the variance; PC2 was related to the volumes of parts, which accounted for 29.81% of the variance; and PC3 was related to the thickness of ICM and TE, which accounted for 13.52% of the variance (Figure 12B). Figure 9A shows plots of PC1 vs. PC2 (a), PC1 vs. PC3 (b), and PC3 vs. PC2 (c). None of the plots clearly separated the P and NP embryos.

Hierarchical Clustering Analysis of the Morphological Parameters of Bovine Blastocysts

The hierarchical clustering analysis based on the blastocoel-related and ZP-related parameters (Figure 13) showed two clusters with a threshold of Dissimilarity = 2.0, and these clusters were also found separated into low (Cluster 1) and high (Cluster 2) blastocoel volume clusters on blastocoel volume-TE + ZP thickness plane (Figure 14). In Cluster 1, no significant difference was found in any of the 22 parameters between the P and NP embryos (Figure 15), while in Cluster 2, TE volume was significantly lower in the P embryos ($p < 0.05$) (Figure 15, 16). No difference between the P and NP embryos in any of the 22 parameters was common to both clusters (Figures 15, 16).

DISCUSSION

The present study describes the 3D images of bovine embryos at the 2-cell and blastocyst stages obtained by OCT. Blastomere nuclei at the 2-cell stage were also clearly visualized by the same system. At the blastocyst stage, 22 morphological parameters were evaluated based on the 3D OCT images. The transfer of 30 bovine embryos after being imaged by OCT resulted in 15 pregnancies (pregnancy rate: 50%) and 12 births (birth rate: 40%), which was typical for the ET attempts (1–4). Bovine blastocysts appeared healthy after a long-term (over 18 h) capture by OCT for monitoring their micro-scale movements [35]. These results indicate that OCT can be used to evaluate embryos before ET. As described previously, OCT can capture the inside structure of mammalian embryos [32-36]. In addition, the present study has made it possible to quantify several parts of bovine blastocysts including its inside structure, such as the blastocoel, which could not be visualized by conventional microscopy.

A PCA of the measured parameters was unable to find the critical parameters associated with pregnancy. To find the critical parameters for pregnancy, a greater number of transfers of OCT imaged embryos is needed. As bovine embryos expand into blastocysts, the thickness of the ZP decreases [5]. In addition, we detected the blastocoel-related parameters (volume and diameter), which were originally quantified in our recent study by OCT [36]. Thus, we conducted a hierarchical clustering analysis based on the blastocoel-related and ZP-related parameters. The hierarchical clustering analysis (Figure 10) shows two clusters with a threshold of Dissimilarity = 2.0, and these clusters were also found separated into

two clusters with low (Cluster 1) or high (Cluster 2) blastocoel volumes on a blastocoel volume-TE + ZP thickness plane. While no difference common to both clusters were found in any of the 22 parameters between the P and NP embryos, TE volume in Cluster 2 was significantly lower in the P embryos than in the NP embryos. In Cluster 2, blastocoel volumes were relatively high and the TE + ZP thicknesses were relatively low (Figure 11), suggesting that embryos in Cluster 2 were well-expanded. These results imply that a low TE volume could be one of the parameters for selecting embryo for ET especially in well-expanded blastocysts. However, since in Cluster 1, there was no significant difference in TE volume between the P and NP embryos, more precise methods for the quantification of TE-related parameters and/or a combination of parameters based on the increased number of OCT images are needed to find the critical parameters for the evaluation of bovine embryos for ET. Furthermore, embryo evaluation is more effective if the OCT measurements are done in parallel with time lapse imaging to evaluate other developmental landmarks, such as the timing of embryo cleavage, timing of each developmental stage, and evaluating cell number.

The present study imaged blastomere nuclei at the 2-cell stage. Karnowski et al. [34] reported that OCT could visualize not only nuclei but also pronuclei and nucleoli in mouse early embryos and blastocysts. They also used OCT to show time dependent changes in these nuclear architectures [34]. In cattle, TLC analysis has revealed that the time-dependent changes, such as the time of the first cleavage and the subsequent number of blastomeres, and the number of blastomeres at the onset of the lag-phase are useful for selecting embryos with a development potential [4, 12-14]. Since we also visualized binuclear cells in a blastomere at the 2-

cell stage, which is known as a negative indicator for development [45], OCT should also be useful for weeding out poor quality embryos. Previous reports also indicate that morphological indices also help to select high quality bovine embryos [4, 13, 45]. Furthermore, the structure of bovine blastocyst has been precisely quantified in the present study. Together, the above findings suggest that detecting time-dependent structural changes of early-stage bovine embryo by OCT could improve evaluations at the blastocyst stage.

The present study reports the first normal deliveries of calves following the transfer of OCT-analyzed bovine embryos. The present conception rate (50%) and the birth rate (40%) following OCT are typical for ETs, indicating that OCT did not adversely affect ET. Although a PCA was unable to identify the parameters associated with pregnancy, TE-related parameters may be useful for evaluating bovine embryos. At present, OCT imaging should be useful for investigating the time-dependent changes of IVF embryos, and with further improvements, be useful for the selection of high-quality embryos for transfer.

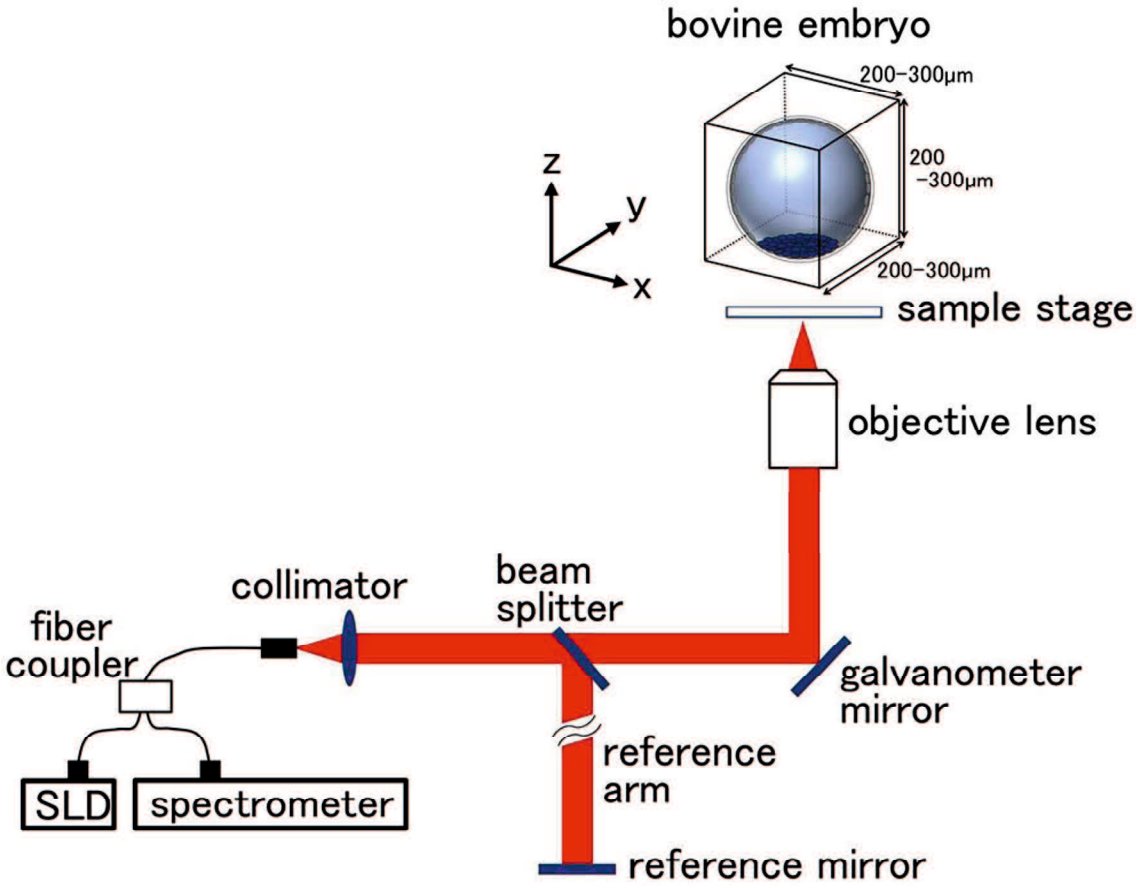

Fig.4 Optical coherence tomography (OCT) setup. The super luminescent diode (SLD) output is coupled into a single mode fiber and split at the fiber coupler into the embryo sample and reference arms. Reflections from the two arms are combined at the coupler and detected by the spectrometer. Scanning scale for the bovine embryo was 200–300μm in each direction. Longitudinal imaging was performed in the area of bovine embryo.

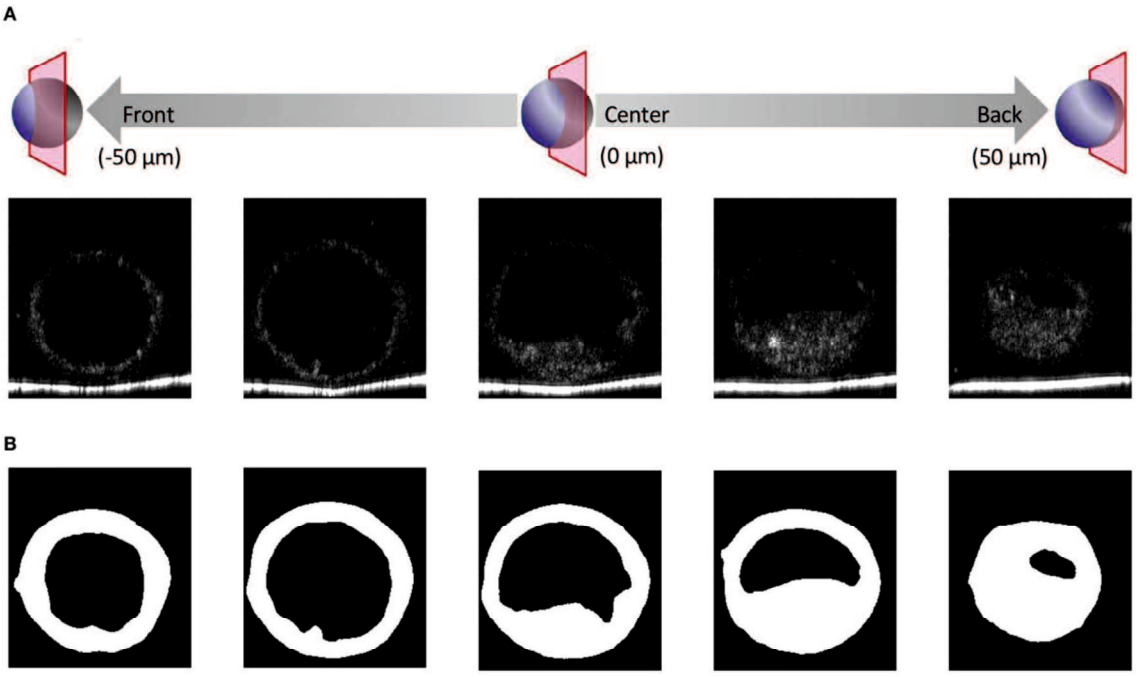

Fig.5 Optical coherence tomography (OCT) images of the bovine embryo and each structure of an embryo. (A) Tomographic images obtained by OCT imaging. Panels are images shifted by 25µm from the center of the embryo. (B) Based on the tomographic images, the structure of the embryo is visualized and binarized.

Fig.6

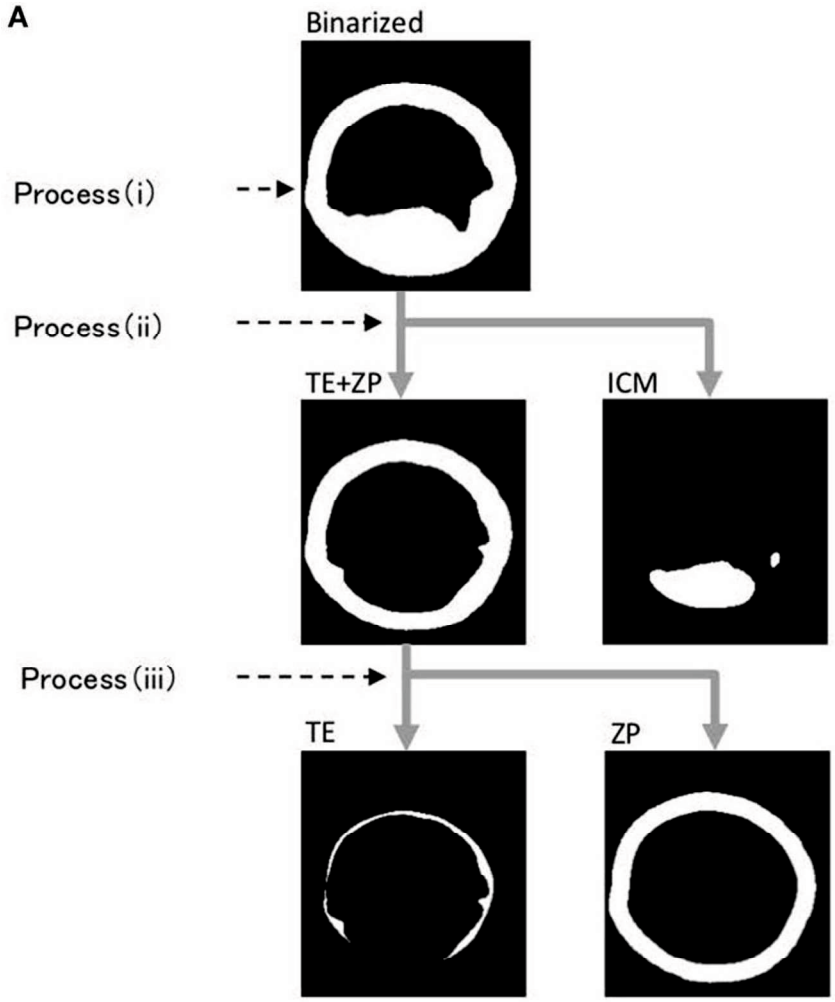

Fig.6 (A) The binarized image was separated into the inner cell mass (ICM), trophectoderm (TE), and zona pellucida (ZP) through processes (i)–(iii).

Fig.6

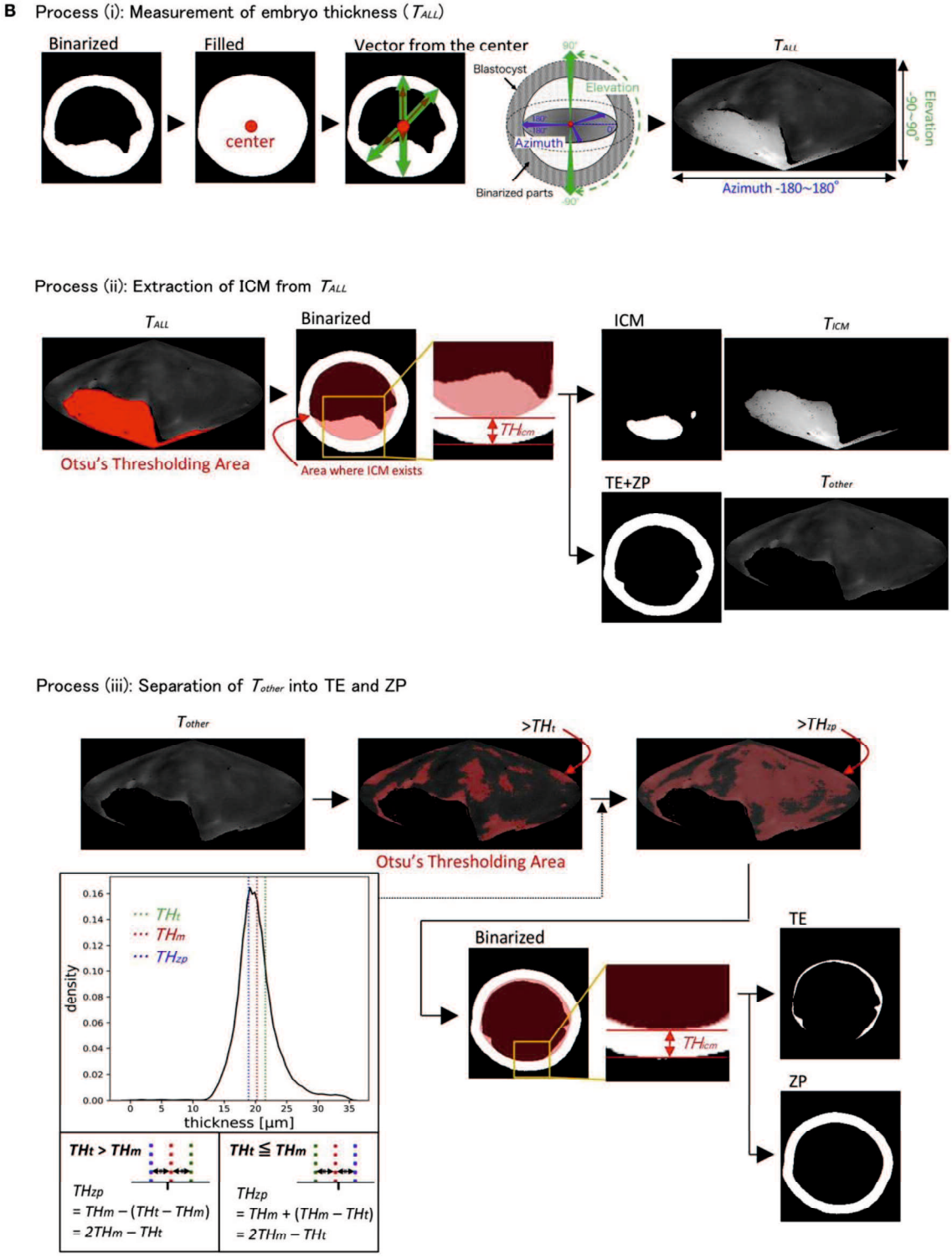
B Process (i): Measurement of embryo thickness (T_{ALL})
Binarized
Filled
center
Vector from the center
Blastocyst
Elevation
Azimuth
Binarized parts
T_{ALL}
Elevation -90~90°
Azimuth -180~180°
Process (ii): Extraction of ICM from T_{ALL}
T_{ALL}
Otsu's Thresholding Area
Binarized
TH_{icm}
Area where ICM exists
ICM
T_{ICM}
TE+ZP
T_{other}
Process (iii): Separation of T_{other} into TE and ZP
T_{other}
$>TH_t$
$>TH_{zp}$
Otsu's Thresholding Area
density
thickness [μm]
TH_t
TH_m
TH_{zp}
Binarized
TH_{icm}
TE
ZP
THt > THm
THzp
= THm − (THt − THm)
= 2THm − THt
THt ≦ THm
THzp
= THm + (THm − THt)
= 2THm − THt

Fig.6 (B) Process (i): Thickness of embryo (T_{ALL}) was measured by drawing vectors from the center to the outer and inner surfaces (the outermost of blastocoel) of the embryo. Process (ii): ICM parts were extracted from T_{ALL} by Otsu's thresholding method (41, 42). Process (iii): The parts, which remained after removing the ICM parts from T_{ALL}, were defined as *Tother*. Tother was separated into TE and ZP by calculating the average thickness of Tother (*THm*) and by using Otsu's thresholding method (41, 42). T_{All}, thicknesses of embryo along each vector; *THicm*, threshold of ICM; T_{ICM}, thickness of ICM; *Tother*, thickness of the areas other than ICM; *THt*, threshold of *Tother*; *THm*, average of *THt*; *THzp*, thickness of ZP (=2 *THm*- *THt*).

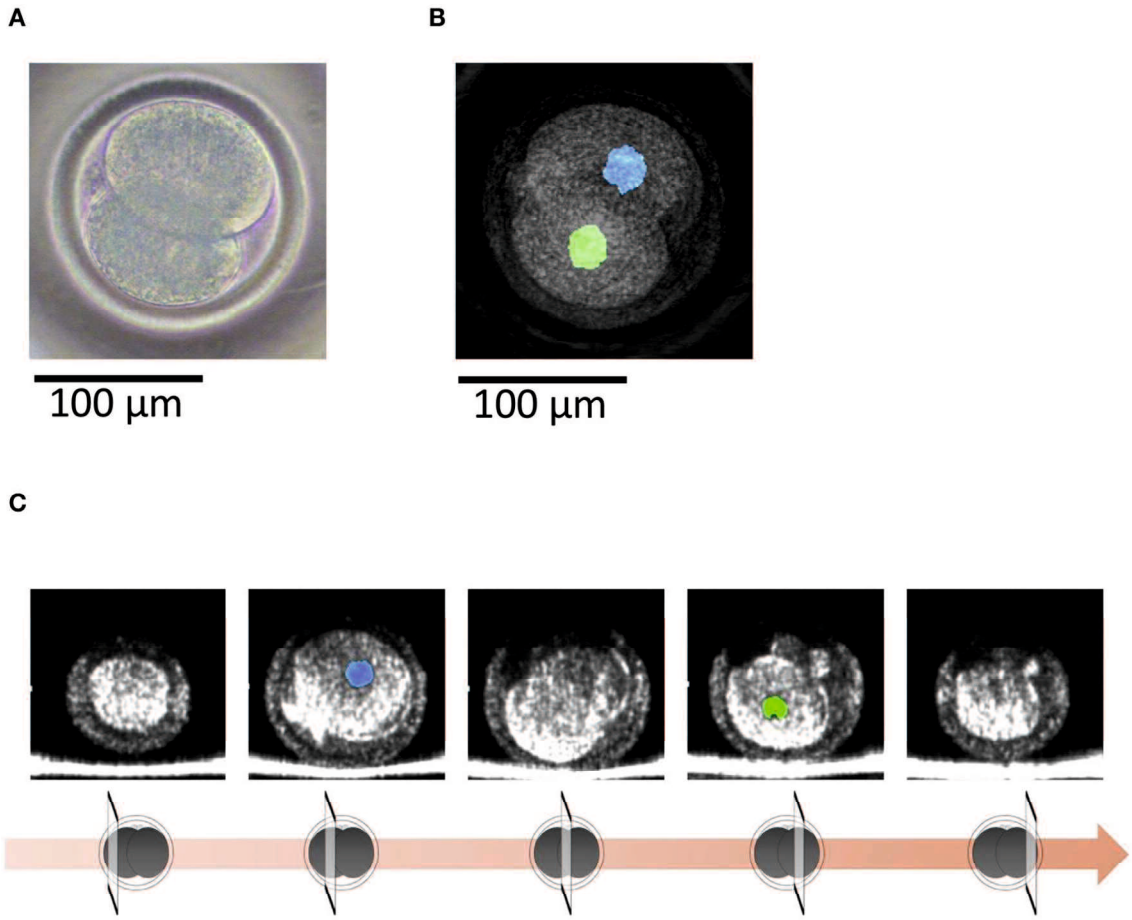

Fig.7 (A) A bovine 2-cell embryo imaged by a microscope. (B) Optical coherence tomography (OCT) images of the bovine 2-cell embryo with visualization of the nucleus (blue and green) of the blastomere. (C) Tomographic images obtained by OCT imaging. Panels are images shifted by 25µm from the center of the embryo with visualization of the nucleus (blue and green) of the blastomere.

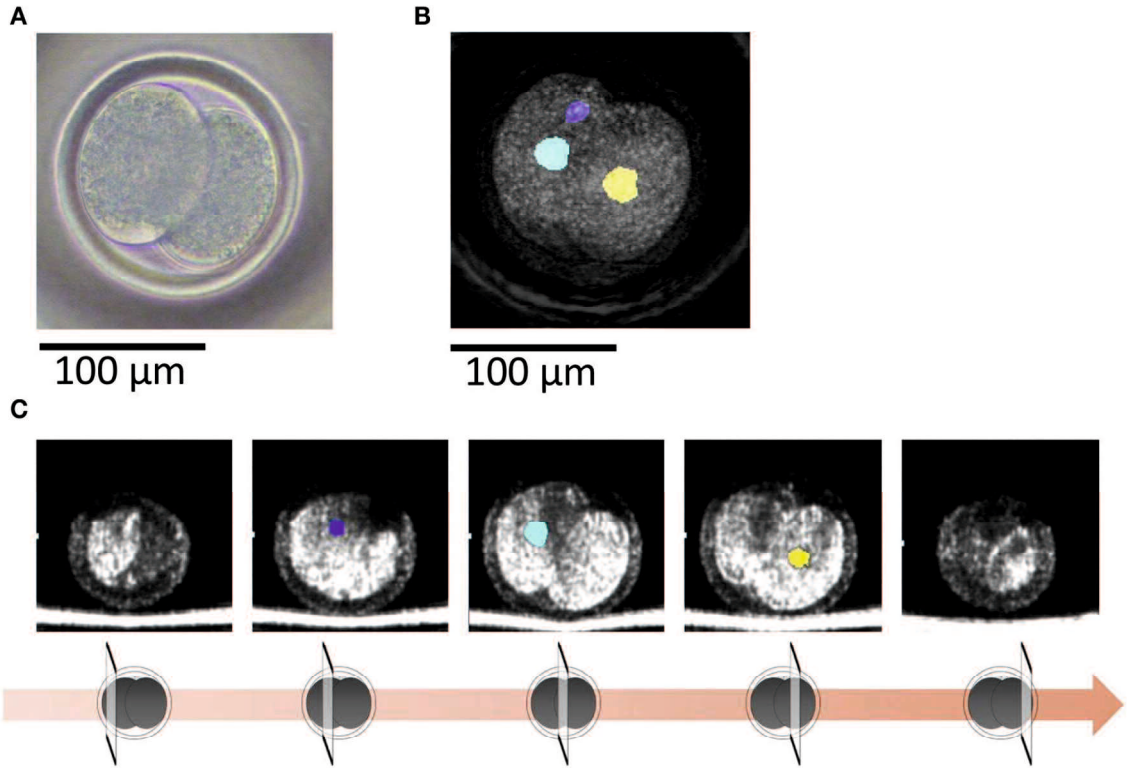

Fig.8 (A) A bovine 2-cell embryo including a binuclear blastomere imaged by a microscope. (B) Optical coherence tomography (OCT) images of the bovine 2-cell embryo including a binuclear blastomere with visualization of the nucleus (blue, green, and yellow) of the blastomere. Blue and green nucleus are in a blastomere. (C) Tomographic images obtained by OCT imaging. Panels are images shifted by 25µm from the center of the embryo with visualization of the nucleus (blue, green, and yellow) of the blastomere.

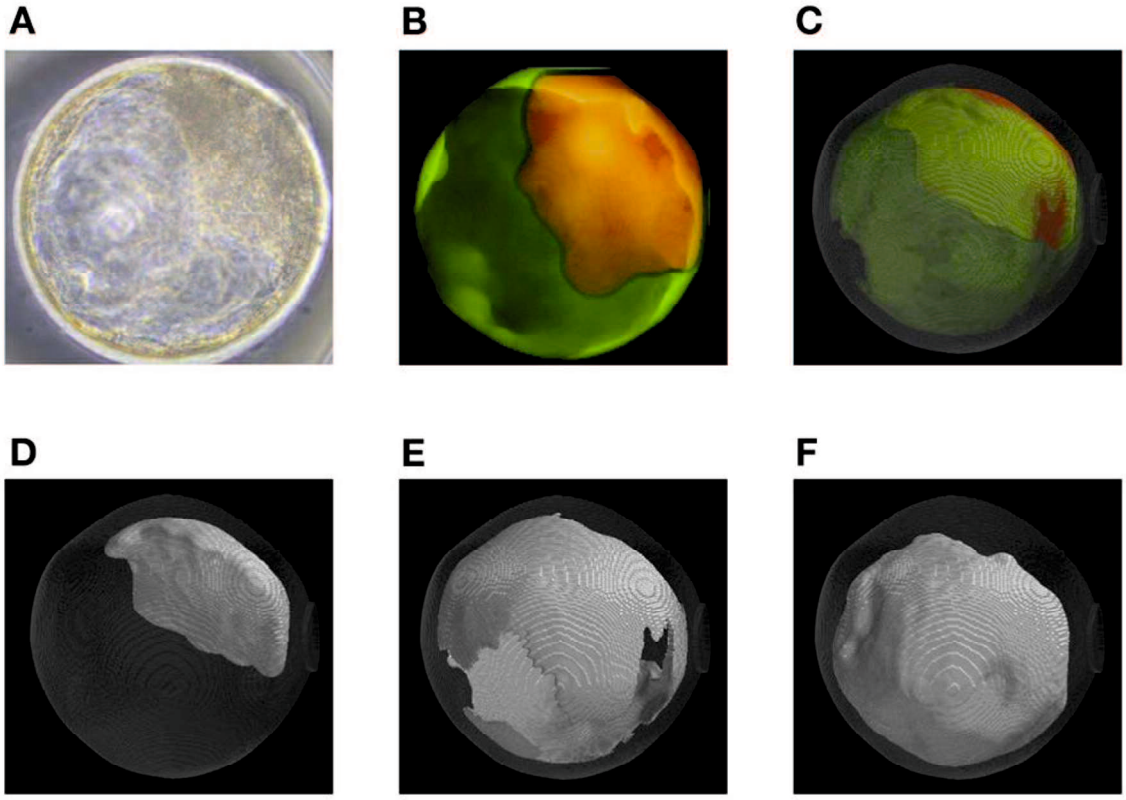

Fig.9 Representative optical coherence tomography (OCT) images of a transferred bovine embryo that resulted in pregnancy. (A) A representative transferred embryo, determined as Code 1 according to the IETS standards, imaged by a microscope. (B) Sum of all pixel values in z-stack images of trophectoderm (TE; bright green) and inner cell mass (ICM; orange) part was extracted from the tomographic image and synthesized 2D image. (C) A 3D-visualization of structures of the embryo, including ICM (orange), TE (bright green), zona pellucida (ZP; gray), and blastocoel. (D–F) A 3D visualization of each structure of the embryo: ICM (D), TE (E), and blastocoel (F). Colors in (B–F) are graphically added.

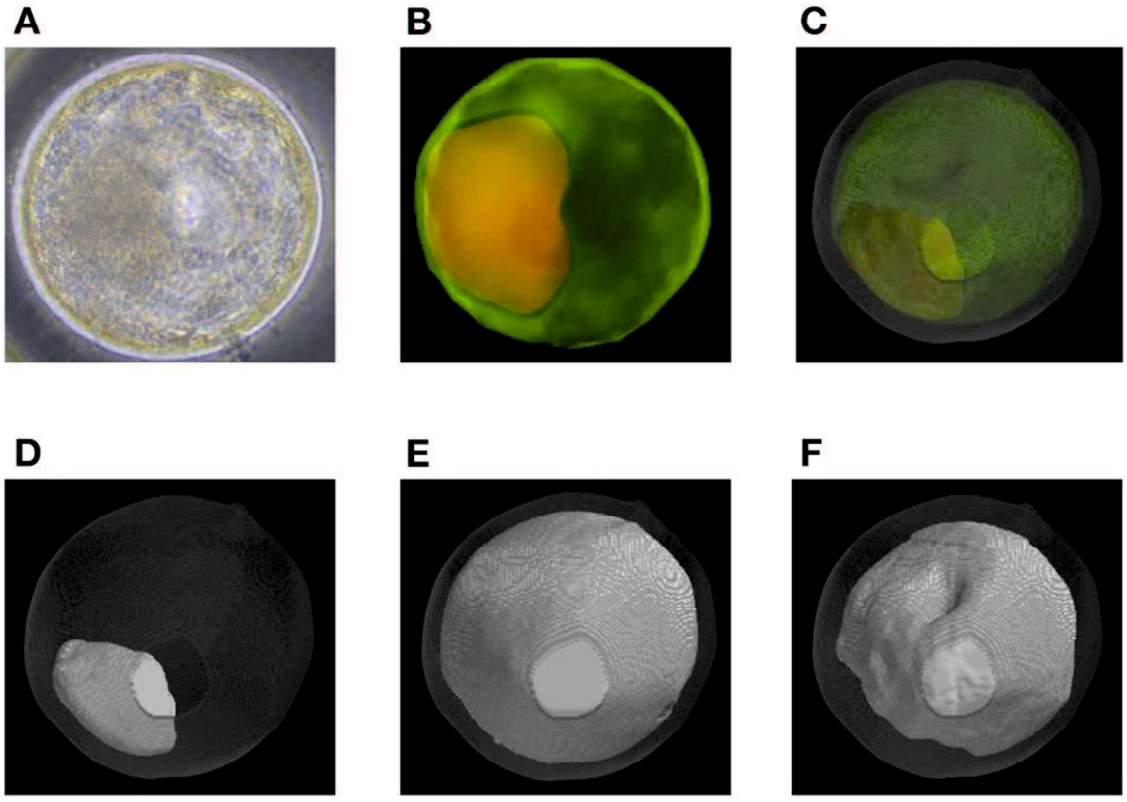

Fig.10 Representative optical coherence tomography (OCT) images of a transferred bovine embryo that resulted in non-pregnancy. (A) A representative transferred embryo, determined as Code 1 according to the IETS standards, imaged by a microscope. (B) Sum of all pixel values in z-stack images of the trophectoderm (TE; bright green) and inner cell mass (ICM; orange) part was extracted from the tomographic image and synthesized 2D image. (C) A 3D-visualization of structures of the embryo, including ICM (orange), TE (bright green), zona pellucida (ZP; gray), and blastocoel. (D–F) A 3D visualization of each structure of the embryo: ICM (D), TE (E), and blastocoel (F). Colors in (B–F) are graphically added.

Fig.11

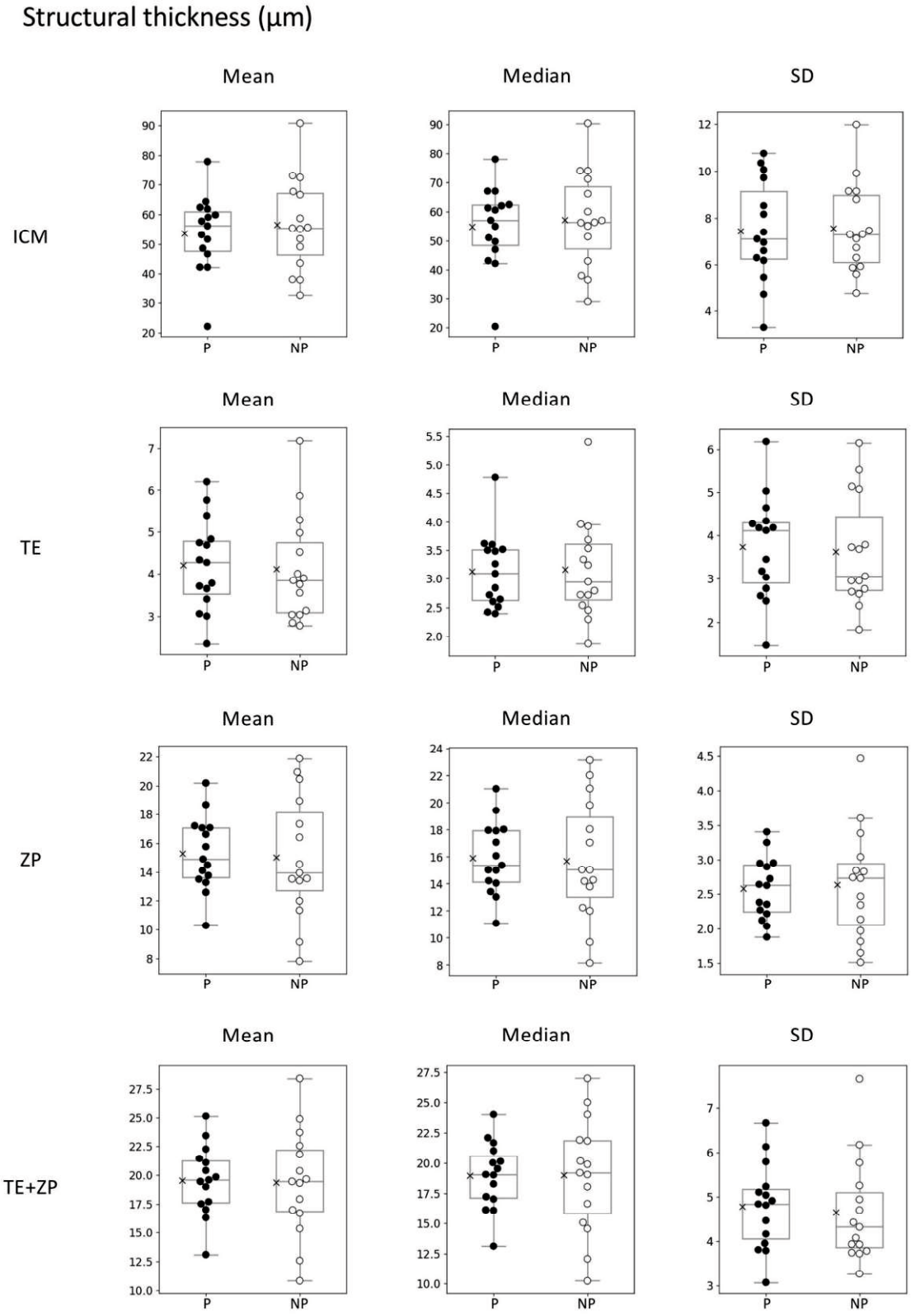

Fig.11

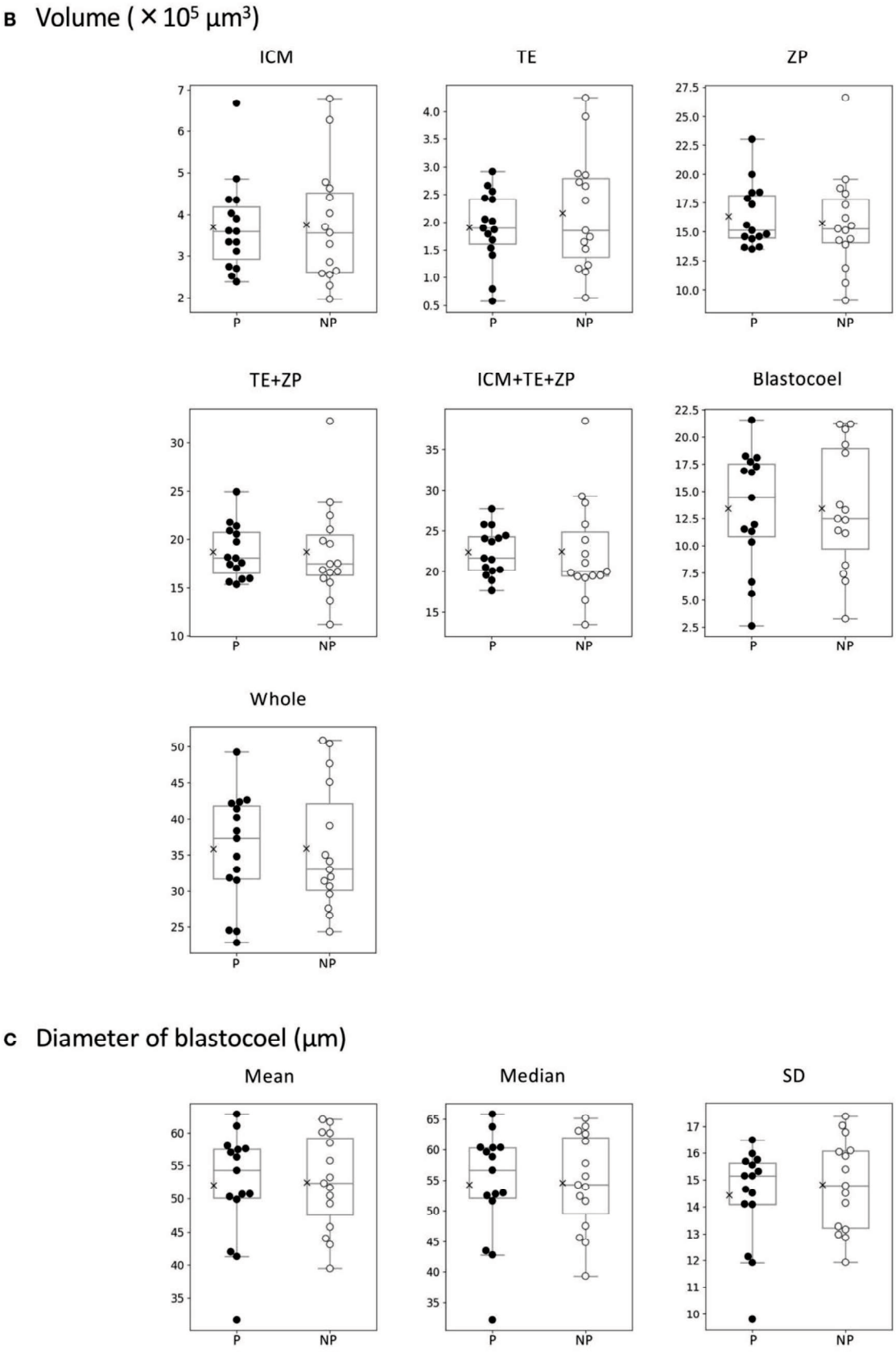
B Volume (× 10^5 μm^3)
ICM
TE
ZP
TE+ZP
ICM+TE+ZP
Blastocoel
Whole
P
NP
C Diameter of blastocoel (μm)
Mean
Median
SD

Fig.11 Comparison of 22 morphological parameters of bovine blastocysts between pregnancy (P: n = 15) and non-pregnancy (NP: n = 15). (A) Parameters related to structural thickness including mean, median, and standard deviation (SD) of inner cell mass (ICM), trophectoderm (TE), zona pellucida (ZP), and TE + ZP. (B) Parameters related to the volume of each part of blastocyst (ICM, TE, ZP, TE + ZP, ICM + TE + ZP, blastocoel, and whole embryo). (C) Parameters related to blastocoel diameter (mean, median, and SD). Statistical significance was analyzed using the Mann-Whitney U test. A value of $p < 0.05$ was considered statistically significant.

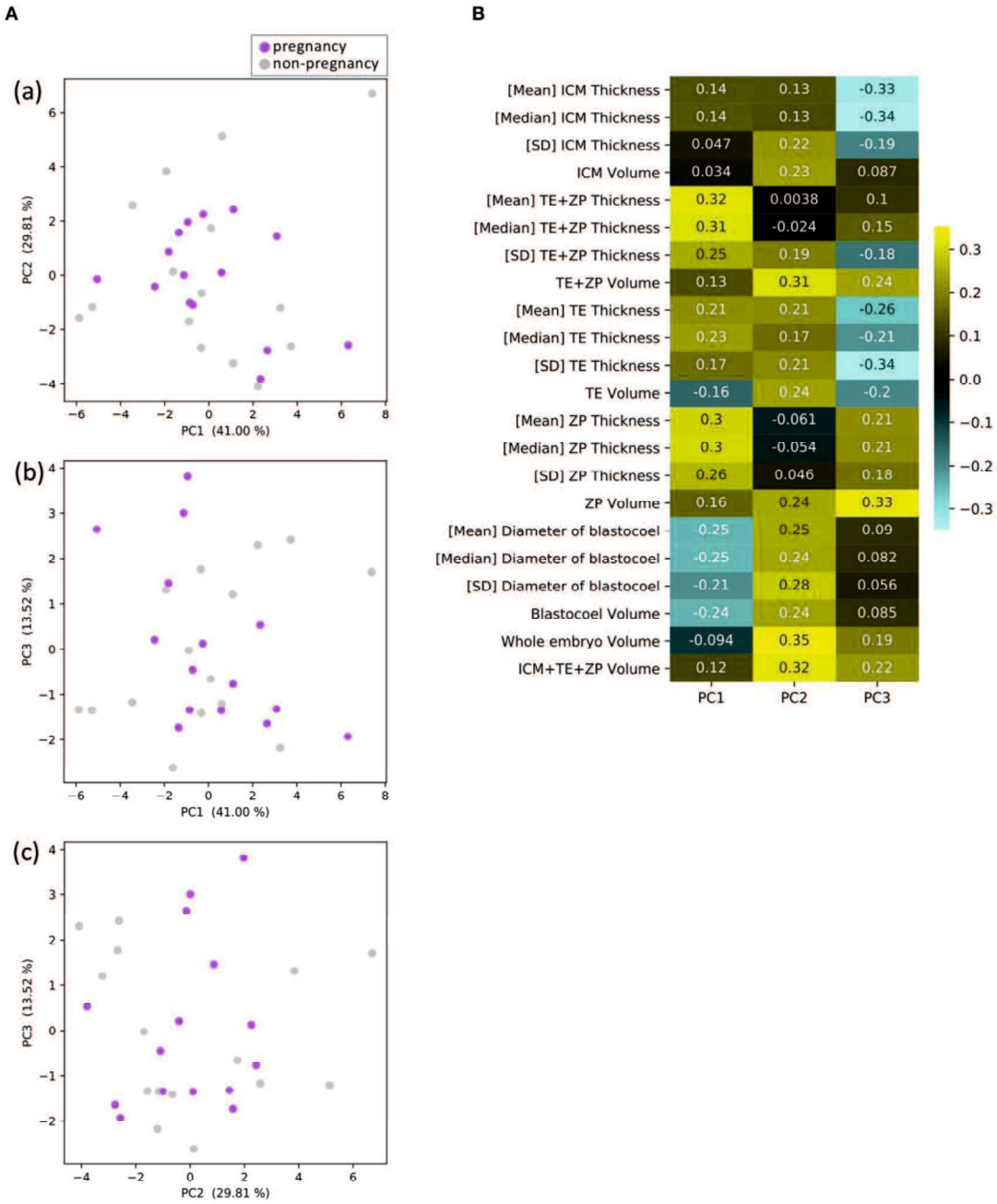

Fig.12 Results of principal component analysis (PCA) based on the 22 morphological parameters of bovine blastocysts (pregnancy: n = 15, non-pregnancy: n = 15). (A) Two-dimensional PCA plots [(a) PC1–PC2, (b) PC1–PC3, (c) PC3–PC2] profiled based on the morphological parameters evaluated from the OCT-scanned 3D images of bovine blastocysts. Each purple and gray dot represents blastocyst resulting in pregnancy and non-pregnancy, respectively. (B) Eigenvectors for PC1, 2, and 3.

Fig.13

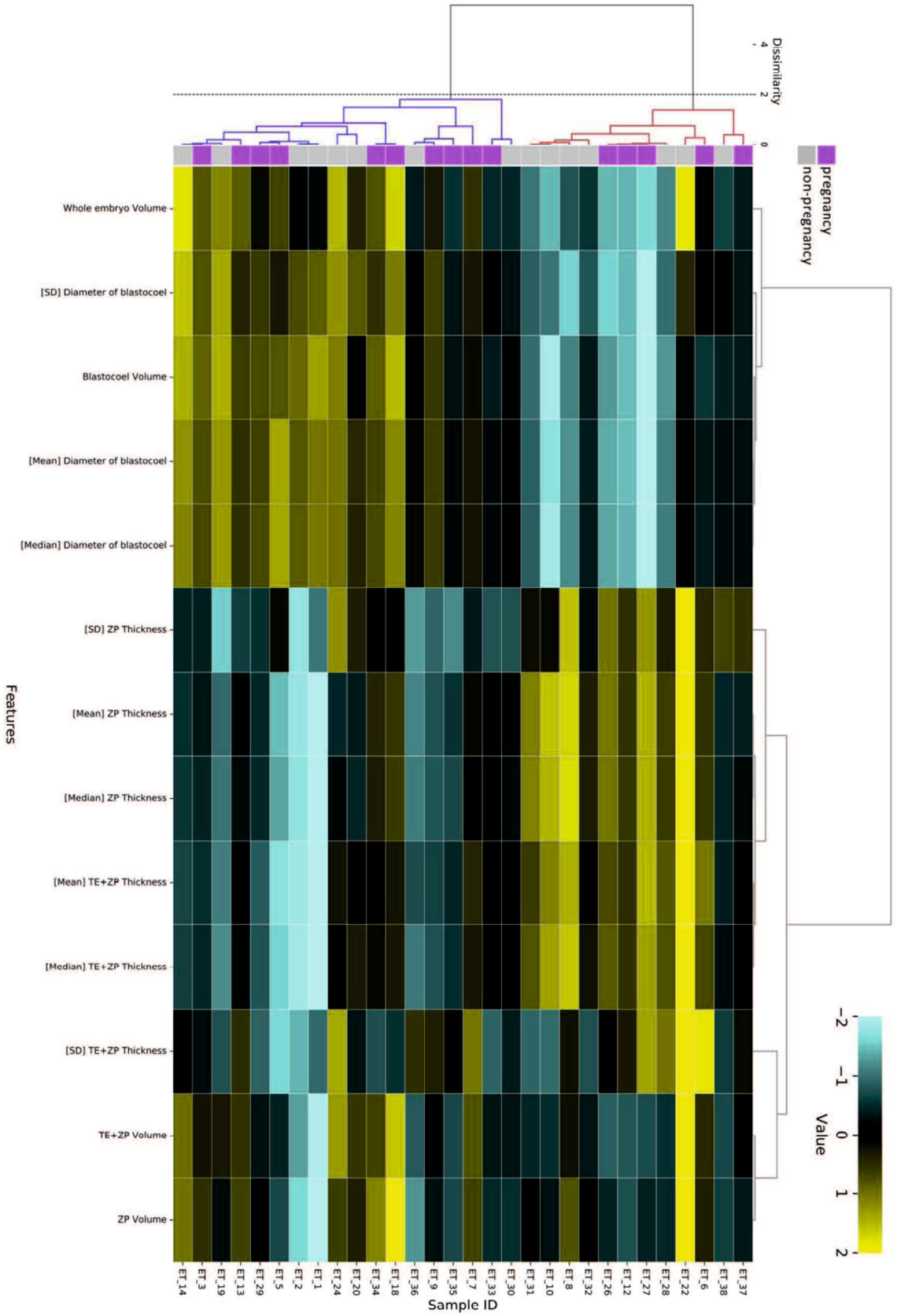
Dissimilarity
4
2
0
pregnancy
non-pregnancy
Whole embryo Volume
[SD] Diameter of blastocoel
Blastocoel Volume
[Mean] Diameter of blastocoel
[Median] Diameter of blastocoel
[SD] ZP Thickness
[Mean] ZP Thickness
[Median] ZP Thickness
[Mean] TE+ZP Thickness
[Median] TE+ZP Thickness
[SD] TE+ZP Thickness
TE+ZP Volume
ZP Volume
Features
ET_14
ET_3
ET_19
ET_13
ET_29
ET_5
ET_2
ET_1
ET_24
ET_20
ET_34
ET_18
ET_36
ET_9
ET_35
ET_7
ET_33
ET_30
ET_31
ET_10
ET_8
ET_32
ET_26
ET_12
ET_27
ET_28
ET_22
ET_6
ET_38
ET_37
Sample ID
−2
−1
0
1
2
Value

Fig.13 Hierarchical clustering analysis performed using 13 blastocoel-related and ZP-related parameters obtained from 30 blastocysts applied for transfer [pregnancy (purple): n = 15, non-pregnancy (gray): n = 15]. Embryos displaying similar patterns for these 13 parameters were grouped together on closely connected branches of the dendrogram with the same color. The color map indicates normalized values that were based on the average value of each parameter (average = 0 and SD = 1). Yellow represents a high value; black represents approximately an equal to average value; and sky blue represents a low value. Metrics and linkage criteria for hierarchical clustering were Pearson's correlation and unweighted average linkage. Two clusters marked with red and blue were obtained with a threshold of Dissimilarity = 2.0.

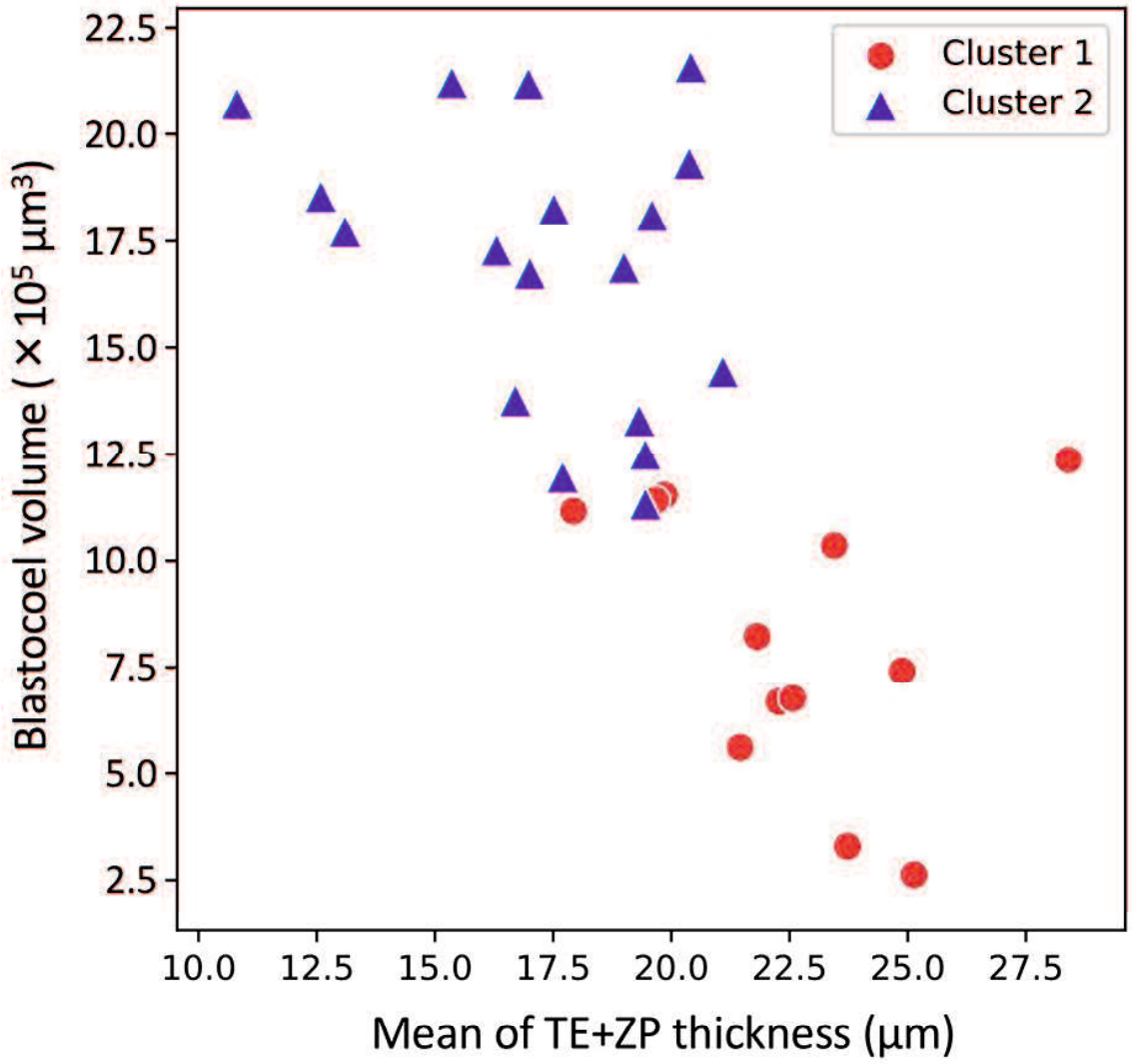

Fig.14 Two-dimensional plots profiled based on the mean of trophectoderm (TE) + zona pellucida (ZP) thickness and blastocoel volume evaluated from the optical coherence tomography (OCT)-scanned 3D images of bovine blastocysts (Cluster 1: red circle, Cluster 2: blue triangle; pregnancy: $n = 15$, non-pregnancy: $n = 15$).

Fig.15 *P*-values in the comparison of 22 parameters evaluated from the optical coherence tomography (OCT)-scanned 3D images of bovine blastocysts between pregnancy and non-pregnancy in each cluster (pregnancy: $n = 15$, non-pregnancy: $n = 15$). Statistical significance was analyzed using the Mann-Whitney *U* test. A value of $p < 0.05$ was considered statistically significant.

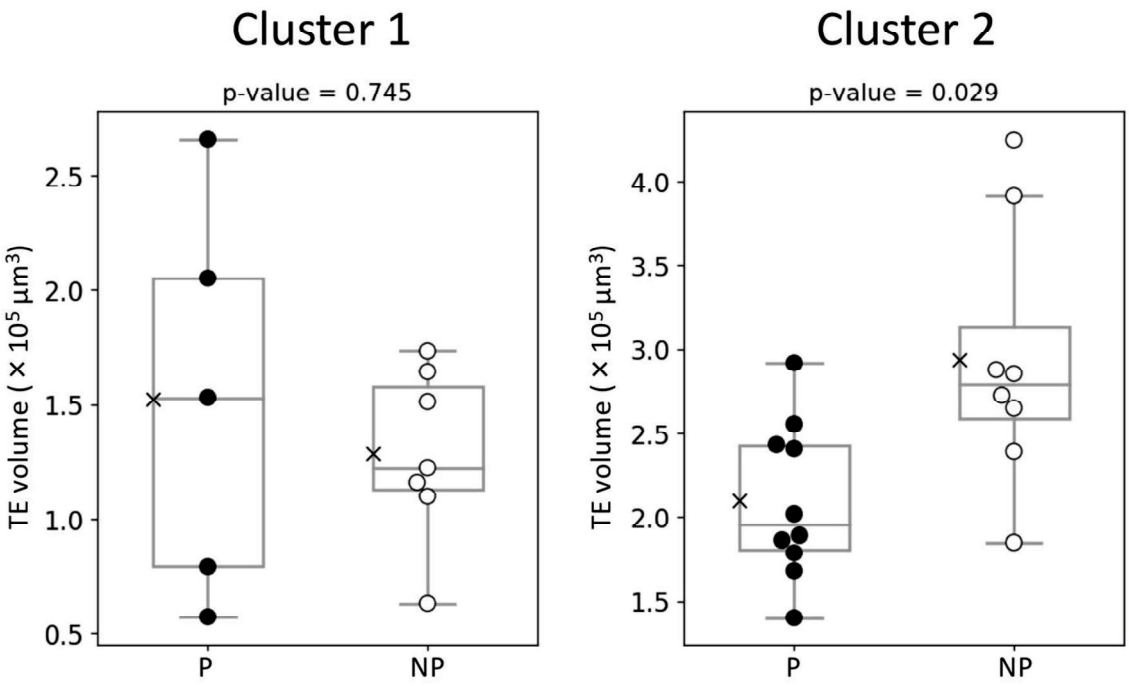

Fig.16 Comparison of TE volume evaluated from the optical coherence tomography (OCT)-scanned 3D images of bovine blastocysts between pregnancy (P) and non-pregnancy (NP) in each cluster (pregnancy: $n = 15$, non-pregnancy: $n = 15$). Statistical significance was analyzed using the Mann-Whitney U test. A value of $p < 0.05$ was considered statistically significant.

Table 2. Quantification of 22 parameters in bovine embryo (Pregnancy: $n = 15$, Non-pregnancy: $n = 15$).

		Pregnancy			Non-pregnancy			*p*-value	$p < 0.05$
		Median	Min	Max	Median	Min	Max		
Structural thickness (μm)									
	Mean	56.2	22.1	77.8	55.4	32.5	90.7	0.7	n.s.
ICM	Median	57.1	20.4	78.1	56.4	28.9	90.4	0.8	n.s.
	SD	7.1	3.3	10.8	7.3	4.8	12.0	1.0	n.s.
	Mean	4.3	2.3	6.2	3.8	2.8	7.2	0.8	n.s.
TE	Median	3.1	2.4	4.8	2.9	1.9	5.4	0.9	n.s.
	SD	4.1	1.5	6.2	3.1	1.8	6.1	0.8	n.s.
	Mean	14.9	10.3	20.2	13.9	7.8	21.9	1.0	n.s.
ZP	Median	15.4	11.1	21.0	15.0	8.1	23.1	1.0	n.s.
	SD	2.6	1.9	3.4	2.7	1.5	4.5	0.9	n.s.
	Mean	19.6	13.1	25.1	19.4	10.8	28.4	1.0	n.s.
TE + ZP	Median	19.1	13.1	24.0	19.2	10.2	27.0	0.8	n.s.
	SD	4.8	3.1	6.7	4.3	3.3	7.7	0.4	n.s.
Volume ($\times 10^5$ μm^3)									
ICM		3.6	2.4	6.7	3.6	2.0	6.8	1.0	n.s.
TE		1.9	0.6	2.9	1.9	0.6	4.2	1.0	n.s.
ZP		15.1	13.5	23.0	15.3	9.1	26.6	0.5	n.s.
TE+ZP		18.1	15.4	25.0	17.5	11.2	32.3	0.5	n.s.
ICM+TE+ZP		21.7	17.7	27.7	20.0	13.4	38.5	0.4	n.s.
Blastocoel		14.4	2.6	21.6	12.5	3.3	21.2	0.9	n.s.
Whole embryo		37.4	22.9	49.3	33.0	24.4	50.9	0.6	n.s.
Diameter of blastocoel (μm)									
Mean		54.3	31.6	62.8	52.3	39.5	62.0	0.8	n.s.
Median		56.7	32.1	65.8	54.2	39.3	65.2	0.8	n.s.
SD		15.1	9.8	16.5	14.8	11.9	17.4	0.8	n.s.

ICM, inner cell mass; TE, trophectoderm; ZP, zona pellucida.

CONCLUSION

The present study is composed of two series of experiments. The first series of experiments described the 3D imaging of bovine embryos by OCT. The 3D images clearly showed the internal structures of bovine embryos, which was difficult to do with a conventional microscope. In addition, the 3D images could be used to quantify morphological parameters, such as thickness and the volume of the parts of embryo including the internal structures. The second series of experiments described 3D images of bovine embryos at the 2-cell embryo and the blastocyst stages obtained by OCT. Furthermore, we transferred 30 embryos captured 3D images by OCT resulting in 15 pregnancies (pregnancy rate: 50%) and 12 births (birth rate: 40%). These results indicate that OCT did not adversely affect ET, and we have firstly reported normal deliveries after transfer of OCT-captured bovine embryo.

The present study was unable to identify parameters associated with pregnancy. Further experiments including a large number of transfers after OCT analyses need to be accumulated to reveal important parameters for bovine embryo evaluation. Generally, this new method has the potential to support the objective evaluation of bovine embryos before ET.

ACKNOWLEDGEMENTS

The author expressed his deep gratitude to Dr. Ryo Nishimura, Associate Professor of Joint Department of Veterinary Medicine, Tottori University, Japan, for his guidance, encouragement, constructive criticism, excellent supervision and for providing the opportunity to conduct this study. I also wish to thank Mr. Ryo Hasebe, Mr. Yasushi Kuromi and Mr. Masayoshi Kobayashi of SCREEN Holdings Co., Ltd, for the providing machines and analyses of this study, and Associate Professor Tetsuya Ohbayashi of Organization for Research Initiative and Promotion, Tottori University, Professor Yoshiaki Yamano, Professor Mitsugu Hishinuma, Professor Yoshiaki Hikasa and Associate Professor Masashi Higuchi of Joint Department of Veterinary Medicine, Tottori University, and Professor Atsushi Asano, Laboratory Animal Science Kagoshima University, for their support, encouragement and advice given at all stage of this study, and Mr. Hikaru Kishida and Ms. Minami Matsuo of Department of Animal Science, Tottori Livestock Research Center, and Ms. Misaki Iwamoto and Ms. Kanako Urataki of Joint Department of Veterinary Medicine, Tottori University, for the technical assistance in providing in vitro embryos for experiments, and the owners and crews of the farms for their outstanding cooperation, and the staff of the Tottori Livestock Research Center for managing donor cows, and the staff of the hygiene centers of Tottori prefecture for collecting of bovine ovaries.

REFERENCES

1. Rizos D, Clemente M, Bermejo-Alvarez P, de La Fuente J, Lonergan P, Gutiérrez-Adán A. Consequences of in vitro culture conditions on embryo development and quality. Reprod Domest Anim 2008;43 Suppl 4:44-50.
2. Lim KT, Jang G, Ko KH, Lee WW, Park HJ, Kim JJ, et al. Improved cryopreservation of bovine preimplantation embryos cultured in chemically defined medium. Anim Reprod Sci 2008;103:239-48.
3. Ferraz PA, Burnley C, Karanja J, Viera-Neto A, Santos JE, Chebel RC, et al. Factors affecting the success of a large embryo transfer program in Holstein cattle in a commercial herd in the southeast region of the United States. Theriogenology 2016;86:1834-41.
4. Sugimura S, Akai T, Imai K. Selection of viable in vitro-fertilized bovine embryos using time-lapse monitoring in microwell culture dishes. J Reprod Dev 2017;63:353-7.
5. Stringfellow DA, Givens MD, International Embryo Transfer S. Manual of the International Embryo Transfer Society : a procedural guide and general information for the use of embryo transfer technology emphasizing sanitary procedures. Savory, Ill.: International Embryo Transfer Society; 2010.
6. Bo GA, Mapletoft RJ. Evaluation and classification of bovine embryos. Anim Reprod 2013;10:344-8.
7. Veeck LL. Oocyte assessment and biological performance. Ann NY Acad Sci 1988;541:259-74.
8. Gardner DK, Schoolcraft WB, Wagley L, Schlenker T, Stevens J, Hesla J. A

prospective randomized trial of blastocyst culture and transfer in in-vitro fertilization. Hum Reprod 1998;13:3434-40.

9. Gardner DK, Meseguer M, Rubio C, Treff NR. Diagnosis of human preimplantation embryo viability. Hum Reprod Update 2015;21:727-47.
10. Yao GD, Xu JW, Xin ZM, Niu WB, Shi SL, Jin HX, et al. Developmental potential of clinically discarded human embryos and associated chromosomal analysis. Sci Rep 2016;6:23995.
11. Tsuiko O, Catteeuw M, Esteki MZ, Destouni A, Pascottini OB, Besenfelder U, et al. Genome stability of bovine in vivo-conceived cleavage-stage embryos is higher compared to in vitro-produced embryos. Hum Reprod 2017;32:2348-57.
12. Sugimura S, Akai T, Hashiyada Y, Aikawa Y, Ohtake M, Matsuda H, et al. Effect of embryo density on in vitro development and gene expression in bovine in vitro-fertilized embryos cultured in a microwell system. J Reprod Dev 2013;59:115-22.
13. Sugimura S, Akai T, Hashiyada Y, Somfai T, Inaba Y, Hirayama M, et al. Promising system for selecting healthy in vitro-fertilized embryos in cattle. PLoS ONE 2012;7:e36627.
14. Sugimura S, Akai T, Somfai T, Hirayama M, Aikawa Y, Ohtake M, et al. Time-lapse cinematography-compatible polystyrene-based microwell culture system: a novel tool for tracking the development of individual bovine embryos. Biol Reprod 2010;83:970-8.
15. Gardner DK, Schoolcraft WB. In vitro culture of human blastocyst. In: Janson R, Mortimer D (eds). Towards Reproductive Certainty: Infertility and Genetics Beyond 1999.Carnforth: Parthenon Press, 1999:378-88.
16. Alpha Scientists In Reproductive M, ESHRE Special Interest Group E. The

Istanbul consensus workshop on embryo assessment: proceedings of an expert meeting. Hum Reprod 2011a;26:1270-83.

17. Alpha Scientists In Reproductive M, ESHRE Special Interest Group E. Istanbul consensus workshop on embryo assessment: proceedings of an expert meeting. Reprod Biomed Online 2011b;22:632-46.
18. Dokras A, Sargent IL, Barlow DH. Human blastocyst grading: an indicator of developmental potential? Hum Reprod 1993;8:2119-27.
19. Shapiro BS, Harris DC, Richter KS. Predictive value of 72-hour blastomere cell number on blastocyst development and success of subsequent transfer based on the degree of blastocyst development. Fertil Steril 2000;73:582-6.
20. Yoon HJ, Yoon SH, Son WY, Im KS, Lim JH. High implantation and pregnancy rates with transfer of human hatching day 6 blastocysts. Fertil Steril 2001;75:832-3.
21. Balaban B, Urman B, Sertac A, Alatas C, Aksoy S, Mercan R. Blastocyst quality affects the success of blastocyst-stage embryo transfer. Fertil Steril 2000;74:282-7.
22. Richter KS, Harris DC, Daneshmand ST, Shapiro BS. Quantitative grading of a human blastocyst: optimal inner cell mass size and shape. Fertil Steril 2001;76:1157-67.
23. Shapiro BS, Richter KS, Harris DC, Daneshmand ST. A comparison of day 5 and day 6 blastocyst transfers. Fertil Steril 2001;75:1126-30.
24. Gardner DK, Lane M, Stevens J, Schlenker T, Schoolcraft WB. Blastocyst score affects implantation and pregnancy outcome: towards a single blastocyst transfer. Fertil Steril 2000;73:1155-8.

25. Zaninovic N, Berrios R, Clarke RN, Bodine R, Ye Z, Veeck LL. Blastocyst expansion, inner cell mass (ICM) formation, and trophectoderm (TM) quality: is one more important for implantation? Fertil Steril 2001;76:S8.
26. Ahlström A, Westin C, Reismer E, Wikland M, Hardarson T. Trophectoderm morphology: an important parameter for predicting live birth after single blastocyst transfer. Hum Reprod 2011;26:3289-96.
27. Nagano M, Takahashi Y, Katagiri S. In vitro fertilization and cortical granule distribution of bovine oocytes having heterogeneous ooplasm with dark clusters. J Vet Med Sci 1999;61:531-5.
28. Jeong WJ, Cho SJ, Lee HS, Deb GK, Lee YS, Kwon TH, et al. Effect of cytoplasmic lipid content on in vitro developmental efficiency of bovine IVP embryos. Theriogenology 2009;72:584-9.
29. Lee E, Takahashi H, Pauty J, Kobayashi M, Kato K, Kabara M, et al. A 3D in vitro pericyte-supported microvessel model: visualisation and quantitative characterisation of multistep angiogenesis. J Mater Chem B 2018;6:1085-94.
30. Pauty J, Usuba R, Cheng IG, Hespel L, Takahashi H, Kato K, et al. A vascular endothelial growth factor-dependent sprouting angiogenesis assay based on an in vitro human blood vessel model for the study of anti-angiogenic drugs. Ebiomedicine 2018;27:225-36.
31. Takahashi H, Kato K, Ueyama K, Kobayashi M, Baik G, Yukawa Y, et al. Visualizing dynamics of angiogenic sprouting from a three-dimensional microvasculature model using stage-top optical coherence tomography. Sci Rep 2017;7:42426.
32. Zheng JG, Lu DY, Chen TY, Wang CM, Tian N, Zhao FY, et al. Label-free

subcellular 3D live imaging of preimplantation mouse embryos with full-field optical coherence tomography. J Biomed Opt 2012;17.7.070503.

33. Zheng JG, Huo TC, Chen TY, Wang CM, Zhang N, Tian N, et al. Understanding three-dimensional spatial relationship between the mouse second polar body and first cleavage plane with full-field optical coherence tomography. J Biomed Opt 2013;18.1.010503.
34. Karnowski K, Ajduk A, Wieloch B, Tamborski S, Krawiec K, Wojtkowski M, et al. Optical coherence microscopy as a novel, non-invasive method for the 4D live imaging of early mammalian embryos. Sci Rep 2017;7:4165.
35. Caujolle S, Cernat R, Silvestri G, Marques MJ, Bradu A, Feuchter T, et al. Speckle variance OCT for depth resolved assessment of the viability of bovine embryos. Biomed Opt Express 2017;8:5139-50.
36. Masuda Y, Hasebe R, Kuromi Y, Kobayashi M, Iwamoto M, Hishinuma M et al. Three-dimensional live imaging of bovine embryos by optical coherence tomography. J Reprod Dev 2021; Apr 21;67(2):149-54.
37. Kikuchi K, Ekwall H, Tienthai P, Kawai Y, Noguchi J, Kaneko H, et al. Morphological features of lipid droplet transition during porcine oocyte fertilisation and early embryonic development to blastocyst in vivo and in vitro. Zygote 2002;10:355-66.
38. Romek M, Gajda B, Krzysztofowicz E, Kepczyn´ski M, Smorag Z. Lipid content in pig blastocysts cultured in the presence or absence of protein and vitamin E or phenazine ethosulfate. Folia Biol 2011;59:45-52.
39. Hidaka T, Fukumoto Y, Yamamoto S, Ogata Y, Horiuchi T. Variations in bovine embryo production between individual donors for OPU-IVF are closely related to

glutathione concentrations in oocytes during in vitro maturation. Theriogenology 2018;113:176-82.

40. Dochi O. Direct transfer of frozen-thawed bovine embryos and its application in cattle reproduction management. J Reprod Dev 2019; 65: 389–96.
41. Otsu N. Threshold selection method from gray-level histograms. IEEE Trans Syst Man Cybern 1979; 9: 62–6.
42. Xue JH, Zhang YJ. Ridler and Calvard's, Kittler and Illingworth's and Otsu's methods for image thresholding. Pattern Recognit Lett 2012; 33: 793–7.
43. Gardner DK, Lane M. Blastocyst transfer. Clin Obstet Gynecol 2003; 46: 231–8.
44. Kragh MF, Rimestad J, Berntsen J, Karstoft H. Automatic grading of human blastocysts from time-lapse imaging. Comput Biol Med 2019; 115: 103494.
45. Yao T, Suzuki R, Furuta N, Suzuki Y, Kabe K, Tokoro M, Sugawara A, Yajima A, Nagasawa T, Matoba S, Yamagata K, Sugimura S. Live-cell imaging of nuclear-chromosomal dynamics in bovine in vitro fertilised embryos. Sci Rep 2018; 8: 7460.
46. Thouas GA, Korfiatis NA, French AJ, Jones GM, Trounson AO. Simplified technique for differential staining of inner cell mass and trophectoderm cells of mouse and bovine blastocysts. Reprod Biomed Online 2001; 3: 25–9.
47. Li R, Pedersen KS, Liu Y, Pedersen HS, Lægdsmand M, Rickelt LF, Kühl M, Callesen H. Effect of red light on the development and quality of mammalian embryos. J Assist Reprod Genet 2014; 31: 795–801.
48. Oh SJ, Gong SP, Lee ST, Lee EJ, Lim JM. Light intensity and wavelength during embryo manipulation are important factors for maintaining viability of preimplantation embryos in vitro. Fertil Steril 2007; 88(Suppl): 1150–7.
49. Pomeroy KO, Reed ML. The effect of light on embryos and embryo culture. J

Reprod Stem Cell Biotechnol 2012; 3: 46–54.

ABSTRACT IN JAPANESE

ウシの受精卵移植技術は、優良な肉用牛や乳用牛の増産・改良のために世界の畜産現場において広く普及している。しかし、人工授精で生産される体内生産胚あるいは体外受精(IVF) で生産される体外生産胚のいずれにおいても移植受胎率は低く、技術の改善が望まれている。ヒトにおける生殖補助医療(ART)では、移植胚は Veeck 分類と Gardner 分類を基準に評価されることが多いが、近年では、タイムラプスシネマトグラフィーを用いた経時的解析が有効な評価方法として用いられつつあり、中でも受精卵の前核もしくは核の数、第一卵割のタイミングや卵割後の割球の数などの指標は ART における着床率の向上に貢献している。一方で、ウシの移植胚は光学顕微鏡を用いた形態観察により国際胚移植学会(IETS)の指標に基づいた品質判定を経て主観的に選別されるのが一般的であり、的確な選別は受胎率を向上させる。この選別には術者の高い選別技術が必要である。こういった現状から、ウシにおける胚移植のさらなる普及にはより効果的かつ客観的な胚の選別手法が求められている。

光干渉断層撮像(OCT)技術は、生体透過性に優れ、非侵襲的に生体内情報を横断断層画像として描出する技術であり、ヒト医療の臨床において眼科の緑内障診断に活用されている。OCT は高い空間分解能で 3 次元 (3D) 画像の観察およびその画像を用いた形態計測が可能な高深度断層撮像システムであり、*in vitro* での血管新生における微細な血管構造を撮像・画像化できることが報告されているが、OCT による胚の画像化に関わる報告は乏しく、ウシ胚の構造を定量化することで胚の品質を評価する手法は報告されていない。本研究では、移植に用いるウシ胚の品質を評価する客観的な手法を確立する目的で、OCT 技術を用いてウシ胚の外部形態と内部構造の非侵襲的な断面画像を撮影し、3D 画像を構築することで複数の形態的パラメーターを定量化することを試みるとともに、撮像胚を移植し、妊娠および分娩について調査した。

第2章では、ウシ移植胚を評価するために、OCT によって撮像した 3D 画像を用いて、生存胚の形態的パラメーターを定量化した。ウシ胚は、黒毛和種から経膣採卵（OPU）にて回収した卵丘卵子複合体（COCs）を用いて IVF によって生産されたものを用いた。実験には、IVF 後 7 日間の培養で拡張胚盤胞に達し、光学顕微鏡下において IETS の指標 Code 1 と分類された 7 胚を用い、OCT による 3D 画像撮像後に移植した。3D 画像から拡張胚盤胞の内部細胞塊（ICM）、栄養外胚葉（TE）、透明帯（ZP）の厚さと体積、および胞胚腔と胚全体の体積を含む 22 のパラメーターを定量化することができた。ICM, TE, ZP および TE + ZP の平均厚はそれぞれ、50.9, 3.8, 14.3 および 18.7 μm であった。ICM, TE, ZP, TE + ZP, ICM + TE + ZP, 胞胚腔および胚全体の体積はそれぞれ、3.2, 3.0, 15.0, 17.4, 20.6, 12.8 および 33.4 × 10^5 μm^3 であった。また、胞胚腔の平均径は 51.7 μm であった。移植した 7 胚のうち 4 胚が受胎したことから、OCT 撮像とその画像をもとに抽出した 22 のパラメーターは、移植に供するウシ胚の品質評価に応用できる可能性が考えられた。

第3章では、ウシ着床前胚の発生能を評価するために、第2章と同様の OCT を用いて 2 細胞期および胚盤胞期の生存しているウシ胚の画像を取得し、ICM の体積や TE の厚さなど、胚盤胞における 22 のパラメーターを定量化するとともに、OCT 撮像後に移植した 30 胚について妊娠診断を実施し、妊娠した例については分娩まで追跡した。ウシ胚は、第2章と同様に作成し、胚盤胞期胚の撮像には IETS 指標の Code 1 に分類されたものを用いた。OCT 画像では 2 細胞期胚の核が明確に観察され、多核割球における核も明瞭に観察された。OCT 撮像後に移植した胚の移植受胎率は 50％（15/30）であり、新生子牛において異常体重や死産は認められず、OCT が移植胚に著しい影響を与えなかったと推察された。主成分分析では、胚の形態的パラメーターの中で受胎に関連するパラメーターの特定には至らなかったが、階層的クラスタリング解析では、一クラスターにおいて、受胎した胚と受胎しなかった胚の TE 体積に有意な差が認められたことから、TE 体積によってウシ胚の品質を評価できる可能性が示唆された。

本研究で確立した OCT を用いたウシ胚形態の定量的評価は、ウシ胚の発育ステージ毎の形態的変化の調査に客観性を付与するとともに、移植に供するウシ胚の客観的な品質評価に役立つことが期待される。